DISSERTAÇÃO DE MESTRADO IFT–D.014/20

Page curve for a perturbed system in 2 dimensional Jackiw–Teitelboim gravity

Sergio Ernesto Aguilar Gutierrez

Supervisor

Nathan Jacob Berkovits

Co-Supervisor

Kyriakos Papadodimas

August 17, 2020

A283p

Aguilar Gutierrez, Sergio Ernesto.
Page curve for a perturbed system in 2 dimensional Jackiw-Teiltelboim gravity / Sergio Ernesto Aguilar Gutierrez. – São Paulo, 2020
48 f. : il.

Dissertação (mestrado) – Universidade Estadual Paulista (Unesp), Instituto de Física Teórica (IFT), São Paulo
Orientador: Nathan Jacob Berkovits
Coorientador: Kyriakos Papadodimas

1. Gravidade (Física). 2. Buracos negros (Astronomia). 3. Ondas de choque. I. Título

Sistema de geração automática de fichas catalográficas da Unesp. Biblioteca do Instituto de Física Teórica (IFT), São Paulo. Dados fornecidos pelo autor(a).

To my parents

Acknowledgements

I would like to thank Kyriakos Papadodimas, who was my supervisor at the ICTP, for instructing me in working on this topic, and teaching me along the way about many foundations on the information paradox and quantum gravity. I am specially thankful to the members of the ICTP in Trieste for allowing me to study the HECAP Diploma program during the thesis year of my master degree, and to the UNESCO for providing me with the financial support during my year in Italy. I was able to take more challenging courses, meet scientists from around the world, and it gave me the chance to work with Kyriakos. Also, thanks to my formal supervisor at the IFT-UNESP, Nathan Berkovits, for teaching me about supersymmetry and string theory, and reviewing this dissertation; although he is one of the busiest members of the IFT-UNESP, he always welcomes questions from his many students, and answers emails quickly. I also acknowledge financial support from the foundations CAPES and FAPESP during the 13 months I studied in Brazil. Thanks to Prem Kumar for a useful discussions.

I could not have made it anywhere without the support and comprehension of my family and friends, thank you.

"We are all like fireworks. We climb, shine and always go our separate ways and become further apart. But even if that time comes, let's not disappear like a firework, and continue to shine... forever."

Tite Kubo, *Bleach.*

Abstract

In this work we review recent developments into a partial solution to the information paradox from context of the Page curve. We study a particular model in 2 dimensional JT gravity coupled to thermal baths, both in an thermal equilibrium and out of equilibrium configurations.

The quantum extremal surface prescription for the computation of the fine grained gravitational entropy is applied in both cases, which leads to the island rule, a spacetime region where we find entropy saddles that restore unitary evolution in the black hole radiation.

For the out of equilibrium case, we review the work of Hollowood-Kumar [1]. We consider the effect of local quenches on the original system, and discover new entropy saddles whose dominance on the Page curve depends strongly on the initial conditions, but they always produce the same late time behavior.

Keywords: Information paradox; Jackiw–Teitelboim gravity; Thermofield double state; Shockwaves; Quantum extremal surfaces.

Knowledge areas: Physics; Black hole physics; Quantum gravity & quantum information.

Resumo

Neste trabalho, revisamos os desenvolvimentos recentes em uma solução parcial para o paradoxo da informação do contexto da curva de Page. Estudamos um modelo específico em gravidade JT bidimensional acoplada a banhos térmicos, tanto em configurações de equilíbrio térmico quanto fora de equilíbrio.

A prescrição da "quantum extremal surface" para o cálculo da entropia gravitacional de granulação fina é aplicada em ambos os casos, que leva à regra da ilha, uma região do espaço-tempo onde encontramos selas de entropia que restauram a evolução unitária na radiação do buraco negro.

Para o caso fora de equilíbrio, revisamos o trabalho de Hollowood-Kumar [1]. Consideramos o efeito de "local quenches" no sistema original e descobrimos novas selas de entropia cujo domínio na curva de página depende fortemente das condições iniciais, mas eles sempre produzem o mesmo comportamento tardio.

Palavras-chave: Paradoxo da informação Gravidade Jackiw–Teitelboim; Thermofield double state; Ondas de choque; Superfícies extremais quânticas.

Áreas de conhecimento: Física; Física do buraco negro; Gravidade quântica e informação quântica.

Contents

Chapter 1

Introduction

This dissertation focuses on recent developments on the computation of the Page curve in JT gravity.

The information paradox has been around since Hawking's findings in the 70's. It appears that a black hole starting in a given quantum state would end up in a state that is not compatible with unitary evolution of quantum mechanics. The most common example is forming a black hole from the collapse of a star which is originally in a pure state, then according to the Hawking calculation, the black hole radiation is thermal and uncorrelated; the final radiation state becomes into a mixed state instead of a pure state that we would expect from the evolution operator; this process would destroy information about the original quantum state.

However, in models where AdS/CFT correspondence is valid provide a counterexample to the possibility of information loss, given that unitarity is present at all stages on the CFT side. It has been conjectured in several instances that information is preserved and that Hawking radiation is not precisely thermal but receives quantum corrections that encode information about the black hole's interior.

This viewpoint received support from the fact that exponentially small corrections to the entropy calculation (those that we can expect from quantum gravity corrections) can lead to a Page curve [2], meaning that the entropy is consistent with unitary evolution. This has been indeed the previous view about entropy evolution in the information paradox before the realization of the island rule. The work of Almheiri et al. [3], and Penington et al. [4] showed that the correct computation entropy of the Hawking radiation does not need small quantum gravity corrections, it arises completely from semiclassical geometry, and it requires that the radiation is in fact dual to certain black hole interior regions (referred as 'islands') which give a relevant entropy contributions at late times, amending information conservation. The island rule has been used to partially solve the AMPS paradox without firewalls [5], which is another relevant puzzle in the information paradox. The island rule and Page curve have been influential in the recent literature; authors have explored different extensions of this machinery, such as: higher dimensional versions of the problem [6]; applications in asymptotically flat gravity models [7, 8], and Schwarzschild black holes [9]; revisiting ideas on baby universes and spacetime wormholes [10]; and the modifications to the Page curve when the systems are perturbed out of equilibrium [1].

Despite the success of the island rule, much more progress needs to be done for achieving a complete solution of the information paradox where quantum information is conserved at all stages of the black hole evaporation. The main difficulty is that the island teach us how to do the entropy calculation correctly but not what are the microscopic degrees of freedom of the Hawking radiation or in the black hole interior, which are involved in the calculation; and also that the procedure has been performed in specific toy models, but it does not mean this would hold for more general configuration, or a realistic black hole system.

In chapter 2 we will review the preliminaries to study the paradox from basic concepts in quantum information; the Hawking calculation for temperature and entropy of black holes, the Bekenstein-Hawking entropy formula (considered as a coarse grained gravitational entropy); we shall state the information paradox, including the Page curve for describing the entropy evolution of a black hole system. Later, the generalized gravitational entropy is introduced, which can be minimized over a quantum extremal surface (QES) to obtain the fine-grained gravitational entropy, i.e. the true entropy used to partially solve the information paradox.

After that, in chapter 3 we present a particular toy model in Jackiw–Teitelboim (JT) gravity that has been used extensively in the literature to study the Page curve problem [11, 12, 3]. We state the characteristics of this model, and the proposed resolution for the entropy curve that is consistent with unitary evolution, from the evaluation of QES. We shall see that as the black hole emits radiation, there is an intrinsic entanglement between the interior geometry of the black hole with its Hawking particles.

In chapter 4, we review a modification of the set up introduced in chapter 3 where shockwaves are inserted in the system, these perturbations take the whole system out of thermal equilibrium until it stabilizes back at late times; and we study how the entropy evolves. This review is motivated to study in a future work, how to produce perturbations around the initial thermal state, and calculate the corresponding Page curve.

Finally, chapter 5 is dedicated to shed some lights in the problems and future work to provide a better solution to the information paradox. In Appendix A we shall provide details about how to obtain the exact solutions to the differential equations that arise when shock waves are introduced as perturbation to the system, and the high temperature limit of the solutions, which was used to simplify the analysis.

Chapter 2

Information paradox and Page curve

In this chapter we review many of the core concepts in the information paradox, in particular the expected entropy curve for a unitary black hole evaporation vs the one that we would find following the Hawking calculation. We shall overview the key difference between the two approaches when introducing the concepts of fine and coarse grained entropies. This chapter has been based in particular from [13] and [5].

2.1 Hawking radiation

2.1.1 Main characteristics

The starting point for stating the information paradox is the Hawking effect. Bekenstein was the first to conjecture that black holes have entropy associated to them and provided an explicit formula which involves the area of their horizon [14, 15], later Hawking derived an explicit mechanism for black holes to radiate, showing that, indeed, black holes have a temperature from their black body radiation distribution, and derived the entropy relation that Bekenstein conjectured [16, 17].

Hawking's original calculation considers semiclassical gravity near the black hole horizon, treating matter fields as quantum mechanical, but keeping the gravity analysis classical, which is a good approximation for large black holes (much larger than the Planck scale) where the curvature of spacetime around the horizon is small. He published the calculations for Klein-Gordon fields, but it can be generalized to other types. He showed that the emitted particles obey a black body thermal distribution attenuated by greybody factors, which is a frequency dependent factor that measures the modification respect to the perfect blackbody radiation. He found the temperature of the attenuated distribution is given by:

$$T_{BH} = \frac{1}{8\pi G_N M} \tag{2.1}$$

in the case of Schwarzschild black holes. An alternative way to perform the calculation is to expand the metric near the horizon, Wick rotate the time component, and identify the periodicity of the euclidean time, for the horizon to be smooth.

As implication, the entropy can be found from $\frac{\partial S}{\partial E} = \frac{1}{T}$ by relating with the surface area of the black hole $A = 4\pi(2G_N M)^2$ for the Schwarzschild case as

$$S_{BH} = \frac{A}{4G_N} \tag{2.2}$$

which and turns out to be a universal result, for any type of black hole of any number of dimensions. (2.2) was first suggested by Bekenstein based on the generalized second law of thermodynamics [15].

The origin of these thermodynamic quantities comes from the conversion of quantum vacuum fluctuations into pairs of particles, some escaping the black hole while others become trapped inside the horizon.

A natural question is how to interpret the black hole entropy from the microscopic point of view; we may consider that black holes emerge from a fine number microscopic degrees of freedom (dictated by the dimension of the Hilbert space). This is the motivation behind the central dogma, which was brought to life from compelling evidence in string theory. We shall follow [5] for the following discussion.

Central dogma: As seen from the outside, a black hole can be described in terms of a quantum system with A$/(4G_N)$ degrees of freedom, which evolves unitarily under time evolution.

Using this hypothesis, the black hole and the whole spacetime around it, up to some surface, can be replaced by a quantum system which interacts with the outside via a unitary Hamiltonian (which is not manifest in the gravity description). The black hole would behave like other isolated thermodynamic systems (except that the interior is surrounded by an event horizon) when we consider the black hole covered by an imaginary surface, which we shall refer as a "cutoff surface".

The central dogma is a statement about the black hole as seen from the outside, there is no statement about the black hole interior, yet. Furthermore, the degrees of freedom entering in the dogma are not manifest in the gravity picture, in fact we would naively think that classically that for a Schwarzschild black hole of a given mass there are infinite possible configurations of its internal degrees of freedom; different approaches to accounting for these degrees of freedom have been discussed but they still remain vague [5].

However, the results on black hole thermodynamics such as (2.1) and (2.2), as well as the results on fine-grained entropies that we will discuss later, are true properties of a theory of gravity coupled to quantum fields and do not require the validity of the central dogma.

2.1.2 Consequences

- Although the thermodynamic black hole entropy (2.2) can be understood from quantum statistical mechanical interpretation, it is yet unknown how to interpret this entropy purely from gravitational point of view without a quantum gravity formulation such as string theory, AdS/CFT, among others.

- On the other hand, since black holes obey a Planck distribution, with greybody factors, the Stefan–Boltzmann law can be applied to learn about the rate of evaporation of black holes. Since $\frac{\mathrm{d}E}{\mathrm{d}t} \propto -T^4$, for the Schwarzschild case we should have:

$$\frac{\mathrm{d}M}{\mathrm{d}t} \propto -(G_N M)^4 \tag{2.3}$$

  which implies that the time of evaporation of a black hole is of order $t_{\text{evap}} \approx G_N^2 M^3$; for example for $M = M_\odot$, $t_{\text{evap}} \approx 10^{63}$ years.

- We must point out that the original derivation by Hawking had a subtlety; he considered the modes through the infalling body into the black hole for calculating the Bogoliubov coefficients; which is not reliable in the semiclassical description since the modes would be blue-shifted and reach trans-Planckian energies. However, Hawking understood that it was only the horizon structure that mattered to initialize the state of the quantum fluctuations, so this blueshift does not affect the calculation, and there are alternative ways to reproduce the results that avoid the trans-Planckian problem, such as the "nice-slide" expansion [18].

- According to the Hawking calculation, $n-$point functions containing modes of Hawking particles and antiparticles can be factorized into products of 2-point functions, plus corrections [19]; which implies that the Hawking radiation is uncorrelated, a fact that we shall employ in the discussion of the information paradox.

2.2 Preliminaries of quantum information

Consider an orthonormal basis $|i\rangle$ with $i = 1, \ldots, N$ for describing states $|\psi\rangle \in \mathcal{H}$, and construct density matrix to describe the statistical state of a quantum system, which is general is given as $\rho = \sum_{ij} c_{ij} |i\rangle \langle j|$ (with the condition $\sum_i c_{ii} = 1$), and in particular for pure states $c_{ij} = c_i c_j^*$, while for mixed states c_{ij} is more general.

A pure state can always be represented as a density matrix $|\psi\rangle \langle\psi|$, but not all density matrices can be represented as $|\psi\rangle \langle\psi|$. A crucial concept for the information paradox is the von Neumann entropy S_{VN}, which is defined for a density matrix ρ, as:

$$S_{VN} \equiv -\operatorname{Tr}[\rho \log \rho] = -\sum_i p_i \log p_i \tag{2.4}$$

where p_i is the probability that the system will access the i-th microstate in its evolution. If we divide a quantum system into subsystems A and B, then $\mathcal{H}_{AB} = \mathcal{H}_A \otimes \mathcal{H}_B$ with $\dim \mathcal{H}_{AB} = \dim \mathcal{H}_A \times \dim \mathcal{H}_B$.

The most general pure state of the full (AB) system can be written as:

$$|\psi\rangle = \sum_{ij} c_{ij} |i\rangle_A |j\rangle_B$$

with $\sum_{ij} |c_{ij}|^2 = 1$. Such states can be factorizable (i.e. $\psi = |\psi\rangle_A |\psi\rangle_B$) or non-factorizable, in which case we say that the systems A, B are entangled. The essence of entanglement is that each particle in a system cannot be described independently of the state of the others.

If $\dim \mathcal{H}_A = m \gg 1$, $\dim \mathcal{H}_B = n \gg 1$, the number of entangled states is much larger than the number of factorizable states when we consider large quantum systems.

In order to describe experiments in A, we do not need to know the state ρ of the full system, in such case a reduced density matrix of A, denoted as $\rho_A = \operatorname{Tr}_B \rho$, is introduced; and observables in A would be given by $\langle \mathcal{O}_A \rangle = \operatorname{Tr}[\rho_A \mathcal{O}_A]$.

The entanglement can be measured in different ways, such as the Renyi entropies, defined as:

$$S_n \equiv \frac{1}{1-n} \log \operatorname{Tr} \rho_A^n$$

which is the most complete basis-independent description of ρ_A since the Renyi entropies are the moments of the its eigenvalue distribution.

Another way is to employ the von Neumann entropy of the reduced density matrix, which is denoted as entanglement entropy

$$S_{EE} = \lim_{n \to 1} S_n = -\operatorname{Tr} \rho_A \log \rho_A.$$

The more entangled particles are, the larger S_{EE}.

On the other hand, for a subsystem A of size $\dim \mathcal{H}_A = m$, the maximal entanglement entropy is given as $\log m$, corresponding to a maximally mixed density matrix.

2.3 Fine grained vs coarse-grained entropy

To apply the previous quantum mechanical concepts to understand the information paradox we must recall that the central dogma tell us that the black hole seemed from the outside behaves like an ordinary quantum system, we do not know about its inside. Thus we need to distinguish between two notions of entropy, that we summarize bellow.

Coarse-grained entropy: It's the thermodynamic entropy of the black hole. It can be obtained by considering a candidate density matrix $\hat{\rho}$ that maximizes the von Neumann entropy

$$S_{\hat{\rho}} = \max_{\hat{\rho}}(-\operatorname{Tr}[\hat{\rho}\log\hat{\rho}]) \tag{2.5}$$

among all states that reproduce the actual values of a set of observables, A_i, that we are keeping track of

$$\operatorname{Tr}[A_i\hat{\rho}] = \operatorname{Tr}[A_i\rho],$$

where ρ denotes the actual density matrix that we have no access to. Explicitly, the coarse entropy that obeys all these properties is given by the maximal generalized entropy, in terms of the area of the horizon plus the contribution from the quantum fields (including gravitons) outside the horizon[20]

$$S_{gen}^{\text{coarse}} = \frac{A}{4G_N} + S_{\text{outside}}. \tag{2.6}$$

By the definition this entropy increases as dictated in the second law of thermodynamics, and has to be larger than the fine grained entropy, so it measure of the total number of degrees of freedom available to the system, and sets the upper bound on the entanglement between the system with something else.

Fine-grained entropy: It's the von Neumann entropy entering in the central dogma; Eq. (2.4) for a given a density matrix ρ. This entropy remains constant under unitary time evolution $\rho \to U\rho U^{-1}$, and it quantifies the ignorance about the precise state of the system, as it vanishes for a pure state (when we know the precise state of the system), and it's non-zero for a mixed state.

In the gravitational case, the fine grained entropy formula is the culmination of several developments on holographic entanglement entropy that we briefly mention. The entropy given as the area of a minimal surface enclosing a region was first proposed in the Ryu-Takayanagi formula, in holographic settings [21]; it was later improved in the Hubeny-Rangamani-Takayanagi formula, which is a covariant generalization that allows time dependence on the entropy [22]; then it was corrected up to one-loop order by Faulkner-Lewkowycz-Maldacena [23], resulting in extra terms that represent the bulk entanglement entropy between regions; and it has been calculated at arbitrary orders using the concept of a *quantum extremal surface* (QES) for minimizing the generalized entropy by Engelhardt-Wall [24].

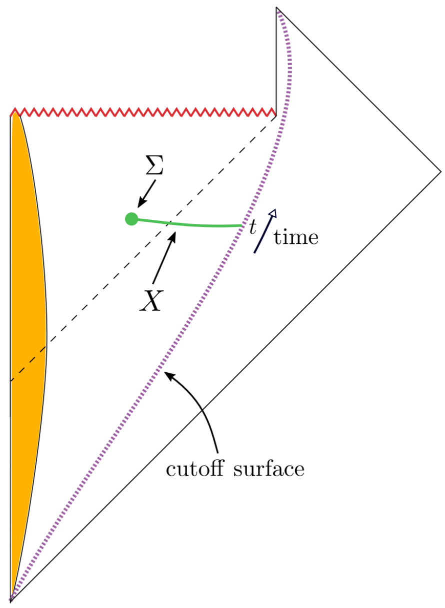

Figure 2.1: QES prescription a evaporating black hole, which is formed by the collapse of a star, and ends up shrinking until disappearing. Σ is the surface that is translated or deformed to extremize the generalized entropy, and X the region between Σ and the cutoff surface appearing in the central dogma.

2.3.1 QES

We shall follow the QES procedure to compute the fine grained entropy S^{fine}. Consider a $(d-1)$-dimensional surface Σ (in a fixed time-slice) in a d space dimensions that minimizes the generalized entropy (area term plus the entropy of fields outside [25]) spatially, but that maximizes it in the time direction:

$$S_{\text{gen}}(X) = \text{min}_{\Sigma}\left\{\text{ext}_{\Sigma}\left[\frac{\text{Area}(\Sigma)}{4G_N} + S_{QFT}(X)\right]\right\} \tag{2.7}$$

where X is the region between Σ and the cutoff region of the gravitational theory, so $S_{QFT}(X)$ is the von Neumann entropy of quantum fields on the interval X. To clarify, in S_{QFT} we are treating the quantum fields (including gravitons) on a classical geometry; so it is calculated by the standard methods of quantum field theory in curved spacetime. Fig. 2.1 shows how to visualize this procedure in the Penrose diagram of a radiating black hole. Although the QES prescription was born from holography, recent developments [3] [4] have shown that the QES arises entirely from semiclassical geometry, from the replica trick method, with the discovery of new saddles in the Euclidean path integral calculation, which are named replica wormholes, that lead to the evaluation of generalized entropy that would had been found with QES.

2.4 Information paradox

Consider star in a pure quantum state collapsing into a black hole. After a long time, the black hole completely evaporates into Hawking radiation which is thermal, so the final state of the quantum system will be a mixed state. This is inconsistent with unitary evolution in quantum mechanics, a pure state remains pure. The same problem could be formulated with an initial mixed state, violation of unitarity would appear. Since the final thermal radiation state only depends on the amount of matter of the black hole, it seems that many initial black hole states lead give the same final radiation state; which implies that information is lost.

Considering the regime where the approximations made by Hawking are valid, there are several possible scenarios for the fate of quantum mechanical information:

- *Information is lost as Hawking predicted*. If pure states evolve to mixed, the foundations of quantum mechanics might need to be modified. Quantum gravity effects should be significant only at the Planck scale, however it might also affect low energy physics via low dimensional operators, which could explain why Hawking's calculation leads to violation of unitarity. However, if this were the case, it can be shown that an initial density matrix of definite energy can evolve into another one where energy conservation is violated in a strong way, which would disagree with observations [26].

- *Information is encoded in the radiation*. The AdS/CFT correspondence shows that information falling into an AdS black hole must be preserved at all stages, providing strong evidence of information conservation, meaning that the radiation encodes information about the black hole's interior. Hawking himself found an unitary mapping from initial to final states in the (asymptotically AdS) black hole formation and evaporation respect to an observer at infinity, by evaluating the Euclidean path integral over different metric topologies [27]. The island rule provides further support for the unitary evolution of black holes radiation, it seems that indeed a pure state returns to pure. Nevertheless, there is much more progress to be done, as the precise way in which information is encoded is not well understood, and there are remaining puzzles (such as firewalls) that have to be resolved to have a complete solution for the paradox.

- *Information is stored in a remnant of the black hole or a baby universe*. In case that a remnant is Planck-sized and stable, we could start with an arbitrarily large black hole and end up with possibly infinite remnants, which will not allow for thermal equilibrium. In case the remnant was large, the black hole would have to stop evaporating before reaching the remnant size, implying a violation of semi-classical gravity. The baby universe case might be a viable possibility, as an observer in our universe would think that information is lost, but instead the black hole S-matrix will depend on the baby universe wavefunction [28]; however, this scenario might not be possible to ever be tested.

2.4.1 Page curve

We could quantify the ideas behind the information paradox by looking at the evolution of entropy of the radiation. Consider that the initial black hole state was in a pure state.

As the black hole radiates, there exist entanglement between the black hole and the Hawking radiation, causing the radiation entanglement entropy to be non-zero during the evaporation, but at the end, when the black hole vanishes, the radiation entropy must decrease back to zero when unitarity is respected, since it corresponds to the entropy of a pure state.

However, the evolution of the radiation entropy in the Hawking calculation seems to be increasing all the time. Consider n Hawking particles emitted by the black hole; where these particles are uncorrelated according to Hawking's calculation, as explained at the end of subsection 2.1.2, meaning that $\rho = \rho_1 \otimes \cdots \otimes \rho_n$, then the total $S_{EE}(n) = nS_{EE}(1)$. We are led to believe that the radiation entropy increases until the black hole completely evaporates, and then becomes constant; it seems that there is no way for the final radiation entropy to go back to zero.

Given that at late times quantum gravity effects dominate, we might think that a possible solution to the paradox is that information comes out near the endpoint of evaporation, in such a way as to turn the Hawking radiation back into a pure state when the black hole in an initial pure state has completely evaporated. However, the maximum von Neumann entropy that a black hole can have is given by $A/(4G_N)$, which is the thermodynamic entropy (decreasing as the black hole evaporates). Since we considering that the black hole starts from a pure state, the von Neumann entropy of the radiation and the black hole are equal, it follows that the entropy of the radiation can not be larger than $A/(4G_N)$. Given that the black hole radiates at a rate given in (2.3), the horizon area decreases, and as a result the thermodynamic black hole entropy decreases; we expect that the entropy of the radiation at late times decreases as well.

The expected unitary evolution of the Hawking radiation entropy is illustrated in the Page curve shown in Fig. 2.2 [5] for a generic system. Since Hawking's calculation is a semiclassical result in effective field theory, we expect quantum corrections that in principle could play an important role in the final result. It can be shown, that the difference between the expectation values of an observable A measured by a pure state vs

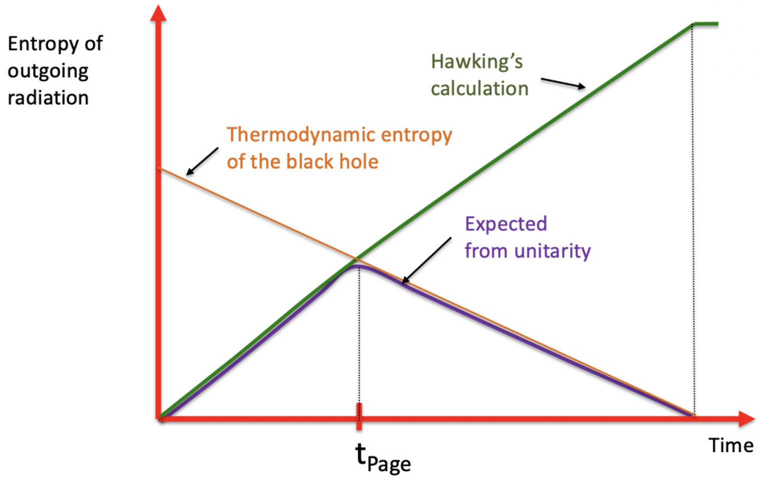

Figure 2.2: Entropy as a function of time where the lines are meant to illustrate monotonic increase or decrease, but the exact shape depends on the details of the gravity theory and matter fields we are considering. The orange line indicates the radiation entropy evolution in the Hawking calculation; while the thermodynamic entropy of the black hole is shown in green, and blue for Page curve, which indicates the minimum entropy between the two cases. The Page curve should be the actual Hawking radiation entropy; the maximum of this curve is found at the Page time t_{Page}.

a maximally mixed state obeys [2]:

$$(\langle\psi| A |\psi\rangle - \text{Tr}[\rho_{\text{mixed}} A])^2 \propto \left(1 + e^S\right)^{-1},$$

which implies that exponentially small quantum corrections (such as quantum gravity effects) are enough for restoring unitarity in large quantum systems. This was indeed one of the main expectations in the scientific community until recently, when researchers were able to reproduce the expected Page curve entirely from semiclassical geometry for certain toy models [3, 4], which is discussed in the following chapters.

2.4.2 Island rule

On the other hand, we could apply the fine-grained gravitational entropy, Eq. (2.7), for the Hawking radiation, as gravity was used to prepare the state of the radiation; specially if the radiation region is entangled with the fields living in the black hole interior. Since the radiation is away from the entangled matter (the fields in the interior of the black hole), then X would be disconnected. Such disconnected region is called an "island" [11, 12, 3, 4, 5], which leads to an increase in the area of the boundary, and a decrease in the semiclassical entropy contribution at the same time. The resulting entropy formula for Hawking radiation is what we will refer to as the "island rule":

$$\boxed{S_{\text{gen}}(\text{Rad}) = \text{min}_{\Sigma}\left\{\text{ext}_{\Sigma}\left[\frac{\text{Area}(\Sigma)}{4G_N} + S_{QFT}(\text{Rad}\cup\text{Isl})\right]\right\}} \tag{2.8}$$

where Σ is the boundary of the island; $S_{\text{gen}}(\text{Rad})$ is entropy of the exact quantum state of the radiation; while the right hand side terms only involve the area of the island, plus the von Neumann entropy of the combined radiation and island systems in the semiclassical description, $S_{QFT}(\text{Rad}\cup\text{Isl})$. This means that although we do not know the exact quantum state of the radiation, we can find its entropy from the semiclassical geometry. In the following chapters, we shall study how this formula reproduces the Page curve for a particular model.

Chapter 3

Page curve in JT gravity

Recently, the Page curve has been computed entirely from semi-classical gravity [11, 3], which partially answers the information paradox without making holographic assumptions. Essentially, the Hawking calculation for the entropy of the emitted radiation is incorrect because it calculates the coarse grained entropy instead of the fine grained one, for which he needed to take into account for an interior region of the black hole that is entangled with the radiation.

Researchers realized that islands regions need to be taken into account to calculate the fine grained entropy, which come from quantum extremal surface calculations of the generalized entropy [12]. The quantum extremal surface prescription has its origins in holography, in particular it was derived from AdS_3 holography for this set up in [11], but it was recently derived without such assumption from the discovery of new saddle points, called replica wormholes, appearing in the path integral calculation of the gravitational entropy [3, 4]. The interpretation of the island region is that this regions inside the black hole are a subsystem of the Hawking radiation.

Although this approach shows how to correctly compute the entropy, the purely semi-classical does not provide any information about the microscopic degrees of freedom encoded in gravity, only their resulting entropy. In other words, the islands allow us to calculate the trace over density matrices of the black hole microstates, from just the semiclassical geometry; resulting in an unitary evolution for the black hole entropy; but it does not provide information about the density matrices themselves.

In this chapter, we review a two dimensional dilaton gravity toy model that has been studied in the recent developments of the information paradox [29, 11, 12, 3, 1], and from which the Page curve was derived, in agreement with unitary evolution of the black hole. This particular set-up allows for many simplifications for the Page curve calculation (such as avoiding the shrinking of the black hole horizon); however other models and generalizations been studied in the literature for the semi-classical calculation of the Page curve, [4, 10, 30, 7, 9].

3.1 The model

3.1.1 Preliminaries

Jackiw–Teitelboim gravity is a theory where the metric is coupled to a scalar (the dilaton, ϕ), and there are no kinetic terms for the scalar. The bulk action in d dimensions for these models contain a term [8]

$$\frac{1}{16\pi G_N}\int d^d x\sqrt{-g}\phi(R-\Lambda),$$

where Λ is the cosmological constant. This choice in the action allows for the metric to remain unchanged at any time by the equations of motion of the dilaton, allowing us to focus on the dynamics of the dilaton instead of the metric.

The model that we discuss for the rest of the dissertation consists on a thermal black hole in AdS_2, where the metric and dilaton are coupled to CFT quantum matter in the gravitational region, and the system is joined smoothly at a boundary to flat space-time where quantum matter is also located, and it acts as a thermal bath. This configuration is illustrated in Fig. 3.2.

An eternal black hole configuration is produced, meaning that shrinking of the horizon is avoided. For this we need to consider that the boundaries between the AdS_2 and Minkowski regions are transparent, i.e. matter can flow freely between the two regions. This allows for the CFT Hawking radiation to be emitted to the thermal baths, and the CFT in the baths passes to the black holes, maintaining thermal equilibrium. If the problem was entirely in AdS space-time, with the usual reflecting boundary conditions, the radiation would eventually fall back into the black hole, making more difficult to study the Page curve.

The action describing this model is as follows:

$$I_{\text{total}} = \frac{1}{16\pi G_N}\left[\int_{\mathcal{M}} d^2x\sqrt{-g}\{\phi_0 R+\phi(R+2)\}+2\int_{\partial\mathcal{M}}\{(\phi_0+\phi_b)K\}\right]+I_{CFT} \tag{3.1}$$

where $\mathcal{M}$ is the spacetime manifold, $R_{\mu\nu}$ the Ricci tensor, ϕ the dilaton, ϕ_0 a constant, and ϕ_b the boundary dilaton.

The variation respect to $g^{\mu\nu}$ and ϕ lead to the equation of motions:

$$(\phi+\phi_0)\left(R_{\mu\nu}-\frac{1}{2}g_{\mu\nu}R\right)=8\pi G_N\langle T_{\mu\nu}\rangle+(\nabla_\mu\nabla_\nu-g_{\mu\nu}\Box)\phi+g_{\mu\nu}\phi, \tag{3.2}$$

$$R=-2 \tag{3.3}$$

respectively, where $T_{\mu\nu} = \frac{-2}{\sqrt{-g}} \frac{\delta I_{CFT}}{\delta g^{\mu\nu}}$.

For the rest of the discussion we shall assume that the central charge c of the CFT is such that $c \gg 1$, needed for the CFT to dominate over quantum gravity effects, allowing for a semi-classical analysis.

3.1.2 Geometry

Eq. (3.3) is used to set the gravity region to a patch of AdS$_2$, with the AdS radius set to 1. Choosing Poincare coordinates, we may express:

$$ds^2_{in} = -\frac{4dx^+dx^-}{(x^+ - x^-)^2} \tag{3.4}$$

where the subindex "in" indicates it's inside the gravity region, which is outside a extremal black hole (zero temperature), the metric diverges at $x^+ = x^-$, but it has no physical singularity since the geometry is locally AdS. The system is coupled to a dilaton (which turns out to be at non-zero temperature as we will see in the next subsection) and a CFT in the AdS$_2$ vacuum state (given that the CFT matter couples to the metric but not to the dilaton). Outside the gravitational region we have a Minkowski spacetime, which can be described by $y^\pm$ coordinates as:

$$ds^2_{out} = -\frac{dy^+dy^-}{\delta^2}; \tag{3.5}$$

where the (spatial) boundary is along the circle $y^\pm = \mp\delta$, for a cutoff parameter δ, which is justified once we extend the $y^\pm$ coordinates to the inside region, and the associated metric in (3.9).

In this model, the geometry can be extended by two half Minkowski space region on the left and right of the Penrose diagram and patched smoothly in the AdS$_2$ geometry [12], [1]. The coordinates that cover the whole space-time, including the black hole interior, are denoted by $w^\pm$, and they are related to the coordinates in (3.4) and (3.5) by the maps:

$$x^\pm = \pm\frac{\beta}{\pi}\frac{w^\pm \mp 1}{w^\pm \pm 1}, \tag{3.6}$$

$$w^\pm = \pm\exp\left[\frac{\pm 2\pi y^\pm_R}{\beta}\right] = \mp\exp\left[\frac{\mp 2\pi y^\pm_L}{\beta}\right] \tag{3.7}$$

respectively; here L, R denote the left and right regions from the black holes in the Penrose Diagram, shown in Fig. 3.1; and β is some fixed constant. $y^\pm_{L,R}$ are an extension of the Minkowski coordinates in Eq. (3.5) for the left and right regions of the diagram, such that $y^+_L - y^-_L \leq 0$, $y^+_R - y^-_R \geq 0$. In the $w^\pm$ coordinates the boundary is now at $|w| = 1 - \frac{2\pi\delta}{\beta}$, where $|w|^2 = -w^+w^-$.

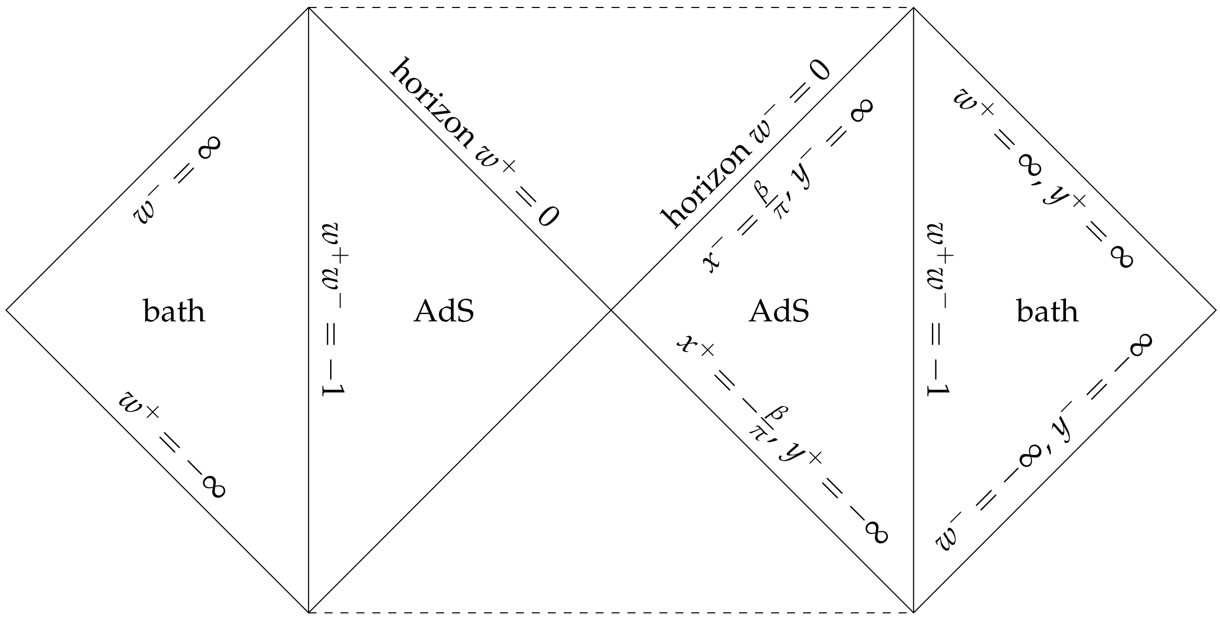

Figure 3.1: Lorentzian picture of two black holes in AdS_2 space time, joined by a Einstein-Rosen bridge, and coupled to thermal baths in Minkowski space-time with transparent boundary conditions.

The $y^{\pm}$ can be extended into the AdS region, covering the outside of the black hole horizon, by the map:

$$x^{\pm} = \frac{\beta}{\pi} \tanh \frac{\pi y^{\pm}}{\beta} \tag{3.8}$$

where, as in Eq. (3.5) we choose $y = y_R$, since we will focus on the right side of the diagram. The $y^{\pm}$ coordinates are denoted "Schwarzschild coordinates" when they map both the AdS (except the black hole) and the Minkowski regions. In the extended $y^{\pm}$ coordinates, we can picture a pair of thermal black holes producing a gravitational region, that is glued to flat space on both sides; a thermal dilaton and CFT matter in a thermofield double state. The metric becomes:

$$ds^2_{\text{in}} = -\frac{4\pi^2}{\beta^2} \frac{dy^+ dy^-}{\sinh^2 \frac{\pi}{\beta}(y^+ - y^-)}, \tag{3.9}$$

where as before, 'in' is the gravity region, and 'out' the matter zone given in Eq. (3.5).

We can write $y^{\pm} = t \pm \sigma$, where t is the boundary time (already discussed in the subsection 3.1.4), and σ is called a "tortoise coordinate" which covers both the gravity and thermal bath spatial regions; $\sigma \leq 0$ for the gravity region, and $\sigma \geq 0$ for the matter region; the boundary at $\sigma = 0$ is where the metric (3.9) diverges, we can introduce the cutoff parameter $\delta \ll \beta$ to shift the boundary, leading to (3.5).

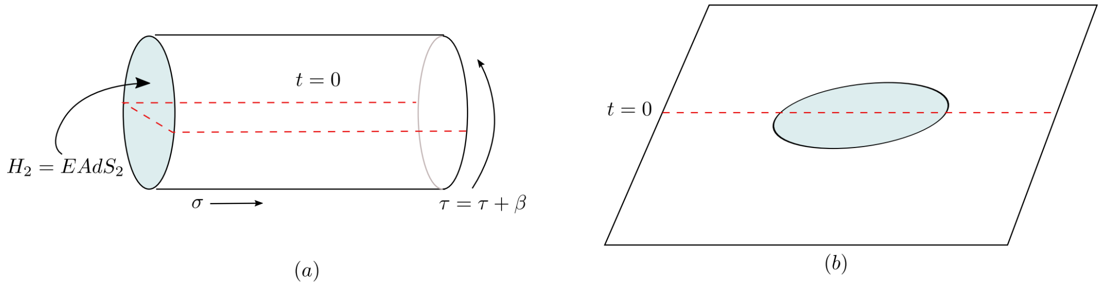

Figure 3.2: Euclidean preparation for thermofield double state of the eternal black hole in AdS and radiation. (a) σ, τ coordinates, forming a cylinder with period β; (b) $x^{\pm}$ coordinates, forming a plane, black hole at zero temperature.

By performing a Wick's rotation $\tau = i\,t$, AdS_2 is identified with the geometry of a cylinder in σ, τ coordinates, with period β, while the patch in $x^{\pm}$ leads corresponds to a plane, with the gravitational region inside a circle, as shown in Fig. (3.2). Since the imaginary time has period β, we see that the metric in (3.9) indeed corresponds to a thermal gravitational region with temperature β^{-1}.

3.1.3 Dilaton solution

The equation of motion of the metric, Eq. (3.2), can be expressed in the $x^{\pm}$ coordinates as:

$$\partial_{x^+}\partial_{x^-}\phi + \frac{2}{(x^+ - x^-)^2}\phi = 8\pi G_N T_{x^+x^-}, \tag{3.10}$$

$$-\frac{1}{(x^+ - x^-)^2}\partial_{x^+}\left((x^+ - x^-)^2\partial_{x^+}\phi\right) = 8\pi G_N T_{x^+x^+}, \tag{3.11}$$

$$-\frac{1}{(x^+ - x^-)^2}\partial_{x^-}\left((x^+ - x^-)^2\partial_{x^-}\phi\right) = 8\pi G_N T_{x^-x^-}. \tag{3.12}$$

This can be simplified if we express $\phi = \phi_{\text{vac}} + \frac{M(x^+,x^-)}{x^+ - x^-}$, where ϕ_{vac} is the sourceless solution, and M is a function that has to satisfy:

$$\partial_{x^{\pm}}\partial_{x^{\pm}}M(x^+, x^-) = -(x^+ - x^-)8\pi G_N T_{x^{\pm}x^{\pm}}(x^{\pm}). \tag{3.13}$$

Integrating the expression, the dilaton solution with $T_{x^+x^-} = 0$ ($T^{\mu}_{\mu} = 0$ can always be imposed by translating the constant $\phi_0 \to \phi_0 + \frac{cG_N}{3}$ [29]) becomes:

$$\begin{aligned}\phi(x^+, x^-) =& 2\phi_r\frac{1 - \frac{\pi^2}{\beta^2}x^+x^-}{x^+ - x^-} + \frac{8\pi G_N}{x^+ - x^-}\int_{x_0^-}^{x^-} dt\,(t - x^+)(t - x^-)T^{(cl)}_{x^-x^-}(t)\\ &- \frac{8\pi G_N}{x^+ - x^-}\int_{x_0^+}^{x^+} dt\,(t - x^+)(t - x^-)T^{(cl)}_{x^+x^+}(t)\end{aligned} \tag{3.14}$$

where ϕ_r is a renormalized boundary value of the dilaton (the dilaton diverges for $x^+ = x^-$), and $x_0^\pm$ indicates initial position. Converting to $y^\pm$ coordinates, in the classical regime where $\langle T_{\mu\nu}\rangle$ is covariant, the AdS_2 vacuum case ($\langle T_{\mu\nu}\rangle = 0$) produces:

$$\phi(y^+, y^-) = -\frac{2\pi\phi_r}{\beta}\frac{1}{\tanh\frac{\pi(y^+-y^-)}{\beta}}. \tag{3.15}$$

At the boundary $\sigma = 0$ ($y^+ = y^-$), the dilaton diverges $\phi|_{\text{bdy}} = \phi_r/\delta$, where δ is a cutoff scale, and "bdy" stands for boundary. We can rescale away this divergence, set $\delta = 0$, consider $y^\pm \to \delta y^\pm$, which changes (3.5) into $ds^2_{\text{out}} = -dy^+dy^-$.

A powerful advantage for choosing this model is that the coarse grained entropy of the black hole can be evaluated as:

$$S_{BH} = \frac{\phi_0 + \phi|_{\text{horizon}}}{4G_N}, \tag{3.16}$$

where the constant ϕ_0 was introduced in Eq. (3.1) just as a shift of the VEV of the dilaton. (3.16) implies that the area for a given surface around the black hole in JT gravity is the same as the dilaton evaluated at the given surface. Notice that Eq. (3.16) follows from evaluating the Euclidean path integral on the disk with circumference β on the classical saddle point, then plug into the thermodynamic formula [31]:

$$Z \sim e^{-I_{cl}}, \qquad S = (1-\beta\partial_\beta)\log Z,$$

where I_{cl} indicates the Euclidean classical action. On the other hand, we need to specify the initial conditions for the CFT matter, to be able to extract expectation values of observables, such as the stress tensor, and from it extract reaction on the dilaton as a result of the equations of motion. At $t = 0$ the CFT state is the thermofield double (TFD) state,

$$|\psi\rangle = \sum_n e^{-\beta E_n/2}\,|\psi_n\rangle_L \otimes |\psi_n\rangle_R\,,$$

respect to the left and right sides of Fig. (3.1) in the $y^\pm$ coordinates (black holes with temperature β), and the CFT is in the AdS_2 vacuum in the $x^\pm$ or $w^\pm$ coordinates (black holes at zero temperature).

3.1.4 Reparametrization

JT gravity can be entirely formulated in terms of a mapping between Poincare and Schwarzschild coordinates, as the dynamics of the so-called "boundary particle" [29]. This is simply a reparametrization between the bulk Poincare time near the boundary u and the physical boundary time t, such that there is a diffeomorphism $u = f(t)$. The location of this physical boundary is specified by the boundary condition on the bulk fields. In our case the boundary is at $\sigma = 0$, where the metric and dilaton diverge according to Eqs. (3.9) and (3.15), and we can introduce a cutoff, δ, as in the previous section:

$$g_{y^+y^-}\Big|_{\text{bdy}} = \frac{1}{2\delta^2}, \quad \phi\Big|_{\text{bdy}} = \phi_b = \frac{\phi_r}{\delta}. \tag{3.17}$$

Thus, the term involving ϕ_b in the action (3.1) is dominant, which reduces to a boundary term, I_{bdy}, given by [29]:

$$I_{bdy} = \frac{1}{8\pi G_N}\int_{\partial M}\phi_b K \rightarrow \frac{\phi_r}{8\pi G_N}\int dt\{f(t), t\}, \tag{3.18}$$

where

$$\{f(t), t\} = \frac{f'''(t)}{f'(t)} - \frac{3}{2}\left(\frac{f''(t)}{f'(t)}\right)^2. \tag{3.19}$$

This action is invariant under $SL(2, R)$ transformations of the boundary particle

$$f(t) \rightarrow \frac{A\,f(t) + B}{C\,f(t) + D}$$

where A, B, C, D are real constants. It's easy to compute the associated conserved charge under time translations $t \rightarrow t + \delta t$ from the Noether procedure on (3.18), leading to the ADM energy:

$$E(t) = -\frac{\phi_r}{8\pi G_N}\{f(t), t\}. \tag{3.20}$$

3.2 Constructing the Page curve

We need to confirm with this toy model that, as Hawking radiation is deposited in the thermal baths, the entangled between radiation and the black hole increases monotonically at early times, by the same argument as in subsection 2.4.1. It follows from the same discussion that the entropy should not grow beyond a $2S_{BH}^{(\beta)}$ in a unitary theory, as the combined state of black hole and radiation is pure, and each of the two black holes is a quantum mechanical system with a coarse-grained entropy $S_{BH}^{(\beta)}$ given by the number of degrees of freedom, describing the black hole from the outside, that are entangled with the radiation. Since the black hole is in thermal equilibrium, its horizon does not shrink, and $A/(4G_N)$ remains constant. From the Page curve analysis, we should find that the radiation takes the minimum entropy between the Hawking calculation and the black hole coarse-grained entropy, so it should increase at early times, but after the Page time, the entropy should become constant, as shown in Fig. 3.3. In contrast, the Hawking curve would continue growing linearly all the time, as we are considering an eternal black hole

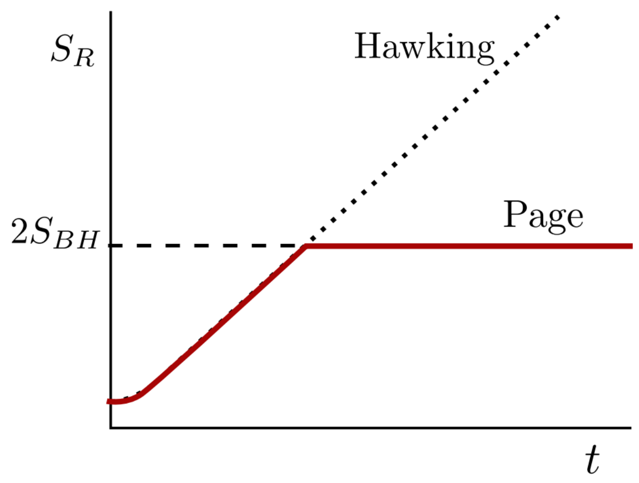

Figure 3.3: Expected Page curve for the JT gravity with quantum matter system in consideration. Dotted line is the Hawking computation, and dashed line is the black hole entropy which is constant in this case since we are considering thermal equilibrium, the solid line is the minimum entropy, creating the Page curve.

system. We shall confirm this behavior by computing the entropy saddles corresponding to no-island and island configurations.

3.2.1 No-island configuration

We proceed to compute entanglement entropy of the bath region, R, respect to the AdS$_2$ region, D, shown in Figure 3.4. Consider a Cauchy slice go across the spacetime passing through the boundary points p_1 and p_2, such that the Hilbert space is factored into $\mathcal{H}_R \otimes \mathcal{H}_D$, because R and D are complementary regions. Since the complete CFT state is pure on a given Cauchy slide: $S(D) = S(R)$, so if we compute $S(D) = -\operatorname{Tr}(\rho_D \log \rho_D)$, we will compute the entropy of the radiation region. We shall identify the coordinates $w_1^{\pm} = \pm e^{\pm 2\pi/\beta}$ on the right boundary and $w_2^{\pm} = \mp e^{\mp 2\pi/\beta}$ on the left; which are chosen since the problem is simple in the coordinate system $w^{\pm}$ where the CFT is in the vacuum respect to the Minkowski metric, $T_{w^{\pm}w^{\pm}} = 0$; while in the original problem $T_{y^{\pm}y^{\pm}} = \frac{c\pi}{12\beta}$ for the coordinate map in Eq. (3.7). There exist an universal result for the entropy of any CFT on a line of squared length $w_{12}^2 \equiv -(w_1^+ - w_2^+)(w_1^- - w_2^-)$ contained between points p_1 and p_2, which is given as [3]:

$$S(R) = S(D) = \frac{c}{6} \log\left(\frac{-(w_1^+ - w_2^+)(w_1^- - w_2^-)}{\Omega_1 \Omega_2 \epsilon_{UV,1} \epsilon_{UV,2}} \right) \tag{3.21}$$

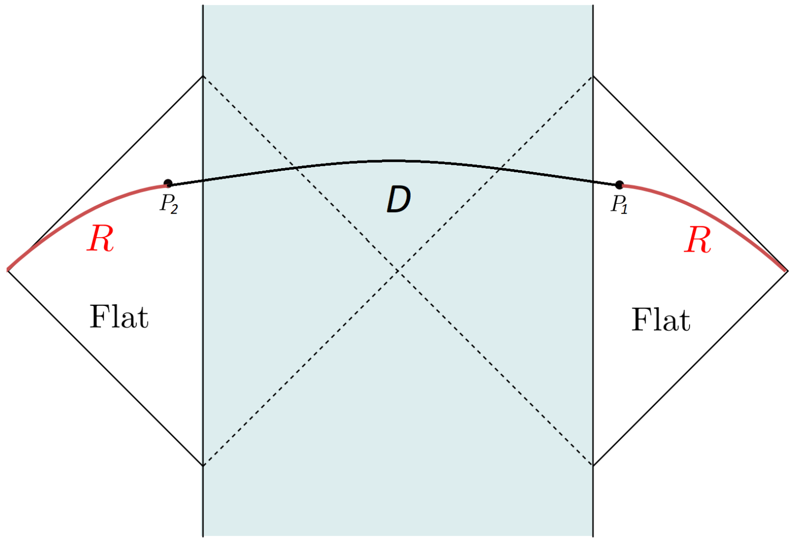

Figure 3.4: No-island saddle. The CFT entanglement entropy for an interval D across the AdS region between boundary points p_1 and p_2 for a given Cauchy surface at a given boundary time t.

where $\Omega_{1,2}$ are conformal factors in $ds^2 = -\Omega^{-2} dw^+ dw^-$, ϵ_{UV} are UV divergences that come in the CFT computation; one cutoff parameter can be absorbed by a rescaling of ϕ_0, and the other can be dropped at some coordinate by a rescaling. Writing explicitly $\Omega^{-2} = \frac{\beta^2}{(2\pi)^2 w^+ w^-}$, and dropping the divergent parameters:

$$S_{\text{gen}}^{\text{no island}} = \frac{c}{3} \log\left(\frac{\beta}{\pi} \cosh \frac{2\pi t}{\beta}\right). \tag{3.22}$$

We see that at late times, $t \gg \beta$, the entropy grows linearly with time:

$$S_{\text{gen}}^{\text{no island}} \simeq \frac{2\pi t}{3\beta}. \tag{3.23}$$

This entanglement entropy increases monotonically since the Hawking radiation is entangled with partner modes behind the horizon, this is the saddle entropy of the Hawking calculation, which naively looks like it would continue forever; however, we shall see that there is another type of saddle which is produces a lower entropy at late time, and it's thus the one that corresponds to the gravitational von Neumann entropy according to the QES prescription; showing that, at least in this model, black holes evaporate following the Page curve.

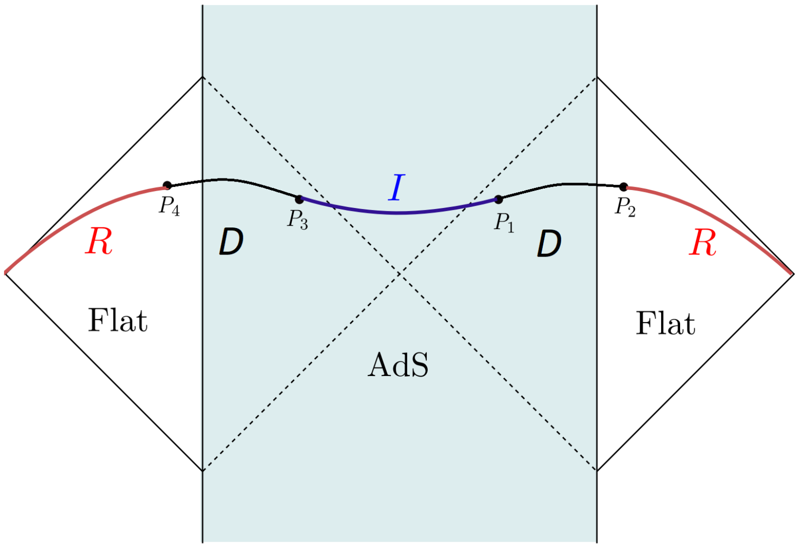

Figure 3.5: Island saddle. p_2 and p_4 are defined to be just outside the boundaries; while p_1 and p_3 are QES in the bulk, which are determined by extremizing the generalized entropy. The radiation region is at $R = [p_4, \infty_L) \cup [p_2, \infty_R)$ and the island at $I = (p_2, p_4)$; D is the complement. We shall compute the generalized entropy resulting from the intervals R and I.

3.2.2 Island configuration

As illustrated in Fig. 3.5, the new saddle produces 2 QES, one on each side, which will turn out to be relevant at late times as they minimize the gravitational entropy. For the model under study, the QES is just a point evolving in time.

The points p_2, p_4 (determining R) and the two QES p_1, p_3 (determining I) are located symmetrically at

$$w_2^{\pm} = w_4^{\mp} = \pm e^{\pm \frac{2\pi t}{\beta}}, \quad w_1^{\pm} = w_3^{\mp}. \tag{3.24}$$

Similar to the no island configuration, in order to compute the generalized entropy for the region $R \cup I$, we can use the fact that the CFT state is pure over a Cauchy slide, so the CFT entanglement entropy can be calculated from the region D:

$$S_{CFT}(R \cup I) = S_{CFT}([p_4, p_3] \cup [p_1, p_2]). \tag{3.25}$$

The von Neumann entropy of a CFT for the union of two disconnected intervals is not universal, contrary to the single interval case that we straightforwardly applied in the no-island case. The entropy will now depend on the cross ratio of the two points on the left and right.

For example, for a theory of c free Dirac fermions, the entanglement entropy of a region $[w_1, w_2] \cup [w_3, w_4]$ with metric $ds^2 = -\Omega^{-2} dw^+ dw^-$ is given by [3]:

$$S_{\text{fermions}} = \frac{c}{6} \log \frac{|w_{21} w_{32} w_{43} w_{41}|^2}{|w_{31} w_{42}|^2 \Omega_1 \Omega_2 \Omega_3 \Omega_4}$$

where $w_{ij} = (w_i^+ - w_j^+)(w_i^- - w_j^-)$. However, at late times ($\frac{2\pi t}{\beta} \gg 1$ in our case) the cross ratio $w_{13} w_{24} / (w_{23} w_{14}) \to 1$ since the left and right contributions decouple and are equal in the OPE limit [3]. This allows us to simplify the discussion if we restrict ourselves to late times, so we will concentrate on the right interval calculation and then double the result. Hence, from the island rule (2.8), the entropy for the Hawking radiation is:

$$S_{gen}(w_1^{\pm}) = 2\left[\frac{\phi_0 + \phi(w_1^{\pm})}{4G_N} + \frac{c}{6} \log\left(\frac{-w_{12}^2}{\Omega_1 \Omega_2}\right)\right] \tag{3.26}$$

where we dropped the divergent quantities, and

$$\Omega_1^{-2} = \frac{4}{(1 + w_1^+ w_2^-)^2}, \qquad \Omega_2^{-2} = \frac{\partial y_2^+}{\partial w_2^+} \frac{\partial y_1^+}{\partial w_1^+} = \left(\frac{\beta}{2\pi}\right)^2.$$

It's useful to rewrite (3.26) as:

$$\begin{aligned} S_{gen}(w_1^{\pm}) = & \frac{\phi_0}{2G_N} + \frac{c}{3} \log \frac{\beta(e^{2\pi t/\beta} - w_1^+)(e^{-2\pi t/\beta} + w_1^-)}{\pi(1 + w_1^+ w_1^-)} \\ & + \frac{c}{3} \frac{\pi}{\beta k} \frac{1 - w_1^+ w_1^-}{1 + w_1^+ w_1^-}, \end{aligned} \tag{3.27}$$

where $k = G_N c / (3\phi_r)$ is the black hole evaporation rate, which we consider in the limit $k \ll 1$ (in units where the AdS radius is 1) for the semiclassical analysis to hold.

In particular, for $k\beta \ll 1$, which is called the high temperature limit, the extremization becomes

$$w_1^{\pm} = -\frac{\beta k}{2\pi w_2^{\mp}} = \pm \frac{\beta k}{2\pi} e^{\pm 2\pi t/\beta} \tag{3.28}$$

which shows that p_2, p_4 would lie on the same Cauchy surface as the QES points p_1, p_3 for a given t; as anticipated in Fig. 3.5. This result also confirms that w_1^- is small (given $\beta k \ll 1$) and negative, so the QES is just outside the black hole horizon.

The critical entropy in the $k\beta \ll 1$ limit becomes:

$$S_{gen}^{\text{island}} = \frac{\phi_0}{2G_N} + \frac{\pi c}{3\beta k} + \frac{c}{3} \log \frac{\beta}{\pi} = 2S_{BH}^{(\beta)}, \tag{3.29}$$

as expected by unitary evolution, it's just the thermodynamic entropy of the two black hole system, as we could anticipate from the result (3.28), given that the QES coordinates are very close to the horizon we end up computing twice the black hole entropy. The result is not just entanglement entropy of R, it's the fine grained entropy, which contains information about the region I behind it.

Thus by the QES prescription, the true entropy of the Hawking radiation as it passes into the auxiliary system is given from by:

$$S(R) = \min\left\{ S_{gen}^{\text{island}}, S_{gen}^{\text{no island}} \right\} \tag{3.30}$$

where the no-island contribution is in (3.22), and the island contribution was approximated for large temperature and times in (3.29), which in the general case it depends in the choice of the CFT matter. However, we see that our computations reproduce the Page curve that we anticipated in Fig. (3.3).

3.2.3 Interpretation around and after Page time

From continuity in the entropy, Eq. (3.23) must coincide with (3.29) at a particular late time, denoted as the Page time:

$$\frac{2\pi}{3\beta} t_{Page} \approx 2S_{BH}^{(\beta)}.$$

An important aspect of the results is whether the fine grained entropy formula can be used to understand how the interior of the black hole encoded in the full Hilbert space; which has been discussed in the context of entanglement wedge reconstruction of AdS/CFT. The entanglement wedge (also called the fine-grained entropy region in [5]) is defined as the causal domain of the region that appears in the computation of the entropy, i.e. the regions bounded between the quantum extremal surfaces and/or cutoff surfaces [29]. The relevant entanglement wedges for the evolution of the system we are considering are represented in Fig. 3.6.

Before, the Page time, there would be an entanglement wedge for the black hole region completely enclosed between p_2 and p_4; and one for the Hawking radiation region. The states and operators in the bulk theory live on a Hilbert subspace of the effective field theory (around the classical background) on a Cauchy slice, called $\mathcal{H}_{\text{code}}$, which in this case can be decomposed as $\mathcal{H}_D \otimes \mathcal{H}_R$, and it can be mapped to a theory living on the boundary.

After the Page time, given the appearance of the two QES in the fine-grained entropy, the entanglement wedge between p_2 and p_4 is cut to end on p_1 and p_3, respectively, leaving a new entanglement wedge in between the two QES, which is what we have been calling an island, I. Given that the island rule reproduces the true entropy that we would expect from the full quantum mechanical prescription, then distinguishable states in the island are distinguishable in the radiation as an exact statement, meaning that states and operators on the island are now encoded by the radiation system rather than the dual boundary

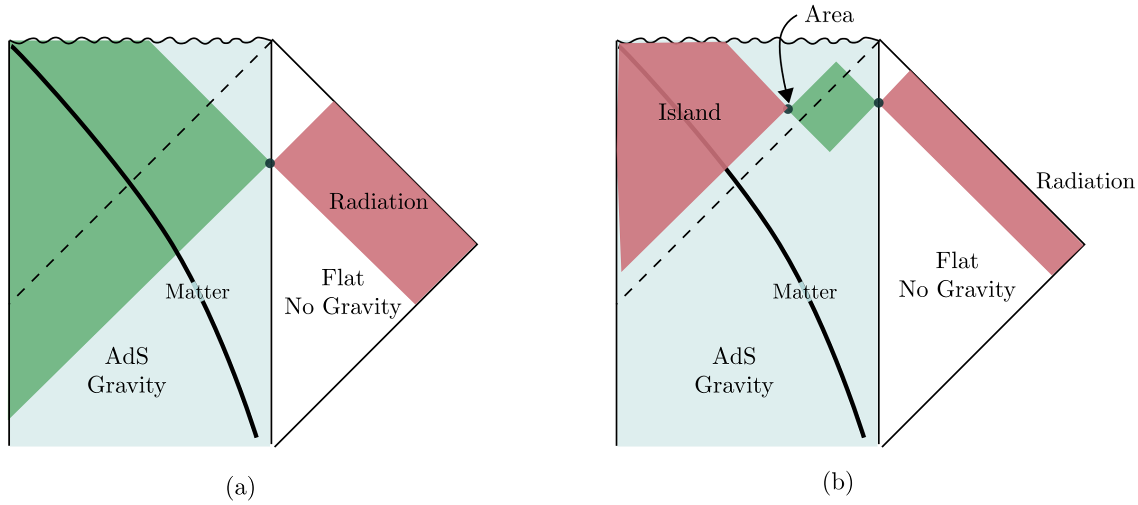

Figure 3.6: One sided picture of the thermal black hole radiating into the flat spacetime region. The red regions denote the entanglement wedge for the radiation and the green ones are the entanglement wedge for the black hole; the black blobs are the QES. (a) At early (boundary) times. (b) At late times. Island regions always exists, but contribute to the entropy after the Page time in our model.

theory, so the $\mathcal{H}_{\text{code}}$ of $R \cup I$ is contained in the full Hilbert space of the radiation. In other words, the degrees of freedom that describe the gravity region only describe a portion of the interior, and the rest of the interior is encoded in the radiation. Some authors [3, 4] have interpreted that as we extract information from the radiation, this process can alter the space time around radiation and create a wormhole that connects to the black hole interior. This arguments are inspired in the interpretation of the ER=EPR conjecture [32].

3.2.4 Relation with the AMPS paradox

Although we have reviewed the island rule for the Page curve computation for a very specific model, we may assume for the sake of the discussion that it holds in more general cases; and study a puzzle related to the Page curve, which is known as the AMPS paradox [33].

Imagine an observer falling into an old black hole that should obey a Page curve. After the Page time, we consider early Hawking radiation, denoted as b' in the Fig. 3.7; later radiation, b; and we denote bb' as the combined system of early and recent Hawking radiation. For the horizon to be smooth respect to the infalling Rindler observer, b must be highly entangled with their partners inside the black hole, denoted as a; which means $S_{ab} \approx 0$, in other words ab is almost a pure state, which implies that $S_a = S_b > 0$ since b is a Hawking particle, in a thermal state.

For a generic quantum system divided into 3 subsystems a, b and b', the strong

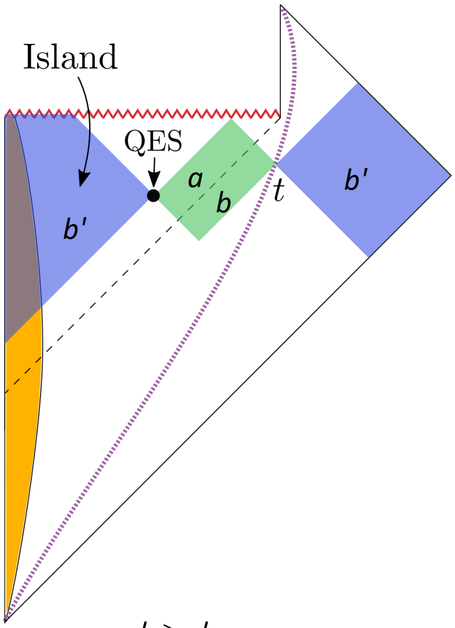

Figure 3.7: The entanglement wedges of a generic black hole and Hawking radiation are shown in green and blue respectively, for boundary times after the Page time t_{Page}. Earlier Hawking radiation is represented as b', b for later Hawking radiation located near the horizon, and a for partner particles of b that are absorbed by the black hole. The diagram considers the island rule, and suggests a solution to the AMPS paradox as a is determined from b'.

subadditivity inequality holds:

$$S_{ab} + S_{bb'} \geq S_a + S_{b'}.$$

In our case, $S_{bb'} > S_{b'}$ (since $S_{ab} \approx 0$), which is what we would expect in the Hawking calculation: the entropy continues growing even after Page time; while if we look at the Page curve, such as the one in Fig. (2.2), we enter into a contradiction as we should have $S_{bb'} < S_{b'}$ at that time.

In the firewall proposal, the way out of the paradox is to avoid the entanglement between particles a, b (for example if virtual particles near the horizon always escape the horizon and become Hawking radiation) then there is no problem with subadditivity, and the infalling observer that crosses the horizon sees no a particles entangled with b. However, when calculating the quantum state in Rindler coordinates and applying it to the expectation value of the stress tensor, it turns out that $\langle T_{\mu\nu} \rangle$ blows up near the horizon [33], the observer would experience something very dramatic instead of what we would expect from the equivalence principle where $\langle T_{\mu\nu} \rangle = 0$ for the Rindler observer, as if it was in the vacuum.

On the other hand, the AMPS paradox has a wrong assumption according to the island rule, the following explanation is based on [5]. The analysis in [33] involved the central dogma, explained in subsection 2.1.1, plus the assumption that all the black hole interior is described by the same degrees of freedom of the black hole seen from the outside. This cannot be true as we have seen, the radiation owns part of the black hole interior degrees of freedom, meaning that the entanglement wedge of the black hole and the radiation are not as simple as assumed in the AMPS proposal. Following figure 3.7, the partner a in the black hole interior is in fact just the future version of the earlier Hawking radiation b', then b is not really maximally entangled with 2 different quantum systems, they are the equivalent; and thus the horizon is smooth, no firewalls are needed.

This explanation sheds light on the unique characteristics of the information paradox. Any statistical system emitting radiation would have a Page curve associated to it, what is special about the process for the black hole is the physics happening at their horizon. Particles carry information about earlier radiation and appear out of the vacuum near the horizon, which itself has no degrees of freedom; so there is nothing on the horizon that can store information. The horizon can be smooth (contrary to firewalls) when the radiation information encoded in the black hole interior.

However, the AMPS paradox is not yet fully solved, as follow up work in [25, 23] raised possible evidence that favor firewall solutions for black holes treated in the AdS/CFT duality, which should be revisited in the light of the island rule.

Chapter 4

Sending perturbations into the black hole

This chapter is a review of [1], where shockwaves are send from the thermal bath of the previous set up. Modifications in the Page curve depend on whether the perturbation was sent before or after the original Page time. The motivation for this chapter is to study in a future work how to apply this procedure to produce perturbations around the TFD state and extract the respective Page curve.

4.1 Producing shockwaves

Shockwaves are pulses of energy that occur when the CFT is perturbed by a local operator, which is a procedure called a "local quench" [34].

In this procedure, the original state $|\psi\rangle$ is modified to $\mathcal{O}(y^+, y^-)|\psi\rangle$, where $\mathcal{O}$ is a primary operator with dimensions $(h, \bar{h})$, and total conformal dimension $\Delta_{\mathcal{O}} = h + \bar{h}$.

The expectation value of an observable can be computed when we consider products that involve both $\mathcal{O}$ and $\mathcal{O}^\dagger$. Our aim is to produce a completely localized CFT excitation from this operators, which would require that both operators are located at the same coordinates. We shall insert the perturbation at the coordinate $y^\pm = t_0$, which is in the thermal bath region, very close to the boundary with the gravitational region.

A convenient way to prepare the local quench is to consider that the operators are slightly separated by an imaginary time parameter ϵ [34, 35], which will turn out to regulate the energy of the perturbation. The operators in the Euclidean picture can be inserted as shown in Figure 4.1, $\mathcal{O}$ at $y_1^\pm = t_0 - i\epsilon$, and $\mathcal{O}^\dagger$ at $y_2^\pm = t_0 + i\epsilon$. The density matrix in the right region of the Penrose diagram, ρ_ϵ, evolves as:

$$\rho_\epsilon(t) = \mathcal{N} e^{-iHt} \mathcal{O}(t_0 + i\epsilon,\, t_0 + i\epsilon) \rho \mathcal{O}^\dagger(t_0 - i\epsilon,\, t_0 - i\epsilon) e^{iHt} \tag{4.1}$$

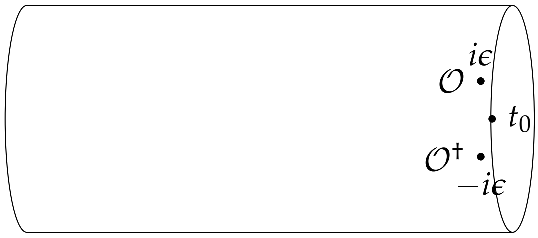

Figure 4.1: In the Euclidean picture, with AdS_2 as a cylinder, we are inserting the operators $\mathcal{O}(t_0 + i\epsilon,\, t_0 + i\epsilon)$, $\mathcal{O}^\dagger(t_0 - i\epsilon,\, t_0 - i\epsilon)$, where ϵ is a temporal width of the pulse that regulates the transferred energy.

where ρ is the original density matrix, $\mathcal{N}$ is a normalization constant, and H is the Hamiltonian.

For the time being ϵ is some arbitrary constant, later we explore a limiting case. The change density matrix implies that expectation values have to be modified, as this is the case for the energy momentum tensor $T_{y^\pm y^\pm}$. We can employ a map from the cylinder to the plane to express:

$$\begin{aligned}\langle T_{y^\pm y^\pm}\rangle_{\mathcal{O}} &\equiv \frac{\langle \mathcal{O}^\dagger(y_1^+, y_1^-) T_{y^\pm y^\pm} \mathcal{O}(y_2^+, y_2^-)\rangle_\beta}{\langle \mathcal{O}^\dagger(y_1^+, y_1^-)\mathcal{O}(y_2^+, y_2^-)\rangle_\beta} \\ &= \left(\frac{\mathrm{d}w^\pm}{\mathrm{d}y^\pm}\right)^2 \langle T_{w^\pm w^\pm}\rangle_{\mathcal{O}} - \frac{c}{24\pi}\{w^\pm, y^\pm\},\end{aligned} \tag{4.2}$$

where β denotes a thermal state; w, w_1, w_2 are the related by (3.7) to y, y_1, and y_2 respectively. Applying standard Ward identities in the plane to evaluate $\langle T_{w^\pm w^\pm}\rangle_{\mathcal{O}}$ and considering $h = \bar{h} = \Delta_{\mathcal{O}}/2$:

$$\begin{aligned}\frac{\langle \mathcal{O}^\dagger(w_1^+, w_1^-) T_{w^\pm w^\pm} \mathcal{O}(w_2^+, w_2^-)\rangle}{\langle \mathcal{O}^\dagger(w_1^+, w_1^-)\mathcal{O}(w_2^+, w_2^-)\rangle} =& \frac{\Delta_{\mathcal{O}}}{2}\left(\frac{1}{(w^\pm - w_1^\pm)^2} + \frac{1}{(w^\pm - w_2^\pm)^2}\right) \\ &- \frac{\Delta_{\mathcal{O}}}{(w^\pm - w_1^\pm)(w_1^\pm - w_2^\pm)} + \frac{\Delta_{\mathcal{O}}}{(w^\pm - w_2^\pm)(w_1^\pm - w_2^\pm)}.\end{aligned}$$

This implies that (4.2) becomes:

$$\langle T_{y^\pm y^\pm}\rangle_{\mathcal{O}} = \frac{\pi c}{12\beta^2} + \frac{2\pi^2\Delta_{\mathcal{O}}}{\beta^2}\frac{\sin^2\frac{2\pi\epsilon}{\beta}}{\left(\cosh\left(\frac{2\pi}{\beta}(y^\pm - t_0)\right) - \cos\frac{2\pi\epsilon}{\beta}\right)^2}, \tag{4.3}$$

which shows that if $\mathcal{O}$ and $\mathcal{O}^\dagger$ were located at the same point, $\langle T_{y^\pm y^\pm}\rangle_{\mathcal{O}}$ would diverge. Taking the limit $\epsilon \ll \beta$ in the previous result:

$$T_{y^\pm y^\pm} = \frac{\pi c}{12\beta^2} + \frac{\Delta_{\mathcal{O}}}{\epsilon}\delta(y^\pm - t_0), \tag{4.4}$$

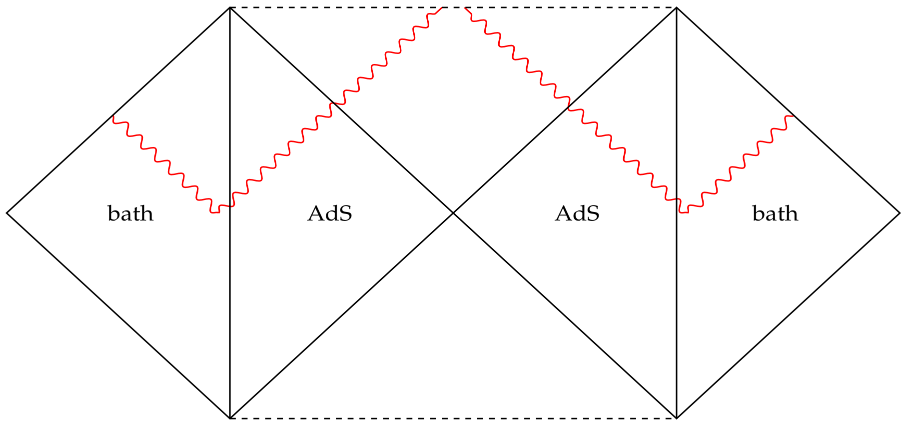

Figure 4.2: Symmetric preparation of energy pulses, shown as red curvy lines, which propagate from the thermal bath, near the boundary, to future null infinity and the interior of black hole. The insertion of the shockwave takes the system out of equilibrium until it stabilizes again.

which shows that in this limit the shockwaves are completely localized in space-time.

The Penrose diagram for this preparation is shown in Fig. (4.2). Integrating the stress tensor (4.4) over space yields the energy carried by a localized shockwave:

$$E_{\text{shock}} = \frac{\Delta_{\mathcal{O}}}{\epsilon}.$$

The operator $\mathcal{O}$ creates entanglement between the left and right moving sectors, providing a shockwave entropy:

$$S_{\text{shock}} = -\sum_a p_a \log p_a = \log d_{\mathcal{O}},$$

where $d_{\mathcal{O}}$ is called the quantum dimension of the operator $\mathcal{O}$ [35].

4.2 Effects of shockwaves

4.2.1 ADM energy

As the shockwave propagates, the ADM mass of the black hole is modified since there is a net flux of energy at the boundary between the AdS region and the thermal bath,

$$E'(t) = T_{y^+y^+} - T_{y^-y^-} \tag{4.5}$$

where $E(t)$ is given in Eq. (3.20), $T_{y^+y^+}$ is the incoming flux by the bath, $T_{y^-y^-}$ the outgoing flux by the Hawking radiation. If there were no shockwaves, the system would be in thermal equilibrium, with $T_{x^\pm x^\pm} = 0$ for the black hole at zero temperature case, also for

$T_{w^{\pm}w^{\pm}} = 0$ since they are related up to a $SL(2, \mathbb{R})$ transformation; and $T_{y^{\pm}y^{\pm}} = \frac{\pi c}{12\beta^2}$ for the thermal case.

The shockwave changes the map in $x^{\pm} = f(y^{\pm})$ from $f(t) = \frac{\beta}{\pi}\tanh\left(\frac{\pi t}{\beta}\right)$ to a different one, which we shall determine from conservation of energy, as follows.

Consider the boundary between the thermal bath and the gravity region after the shock wave was produced, $t > t_0$. The incoming modes contribute to $T_{y^+y^+}$ as given in (4.4), but the outgoing modes (just Hawking radiation) produce $T_{x^-x^-} = 0$. Given the map $x^- = f(y^-)$, we must have:

$$T_{y^-y^-}\Big|_{\text{bdy}} = -\frac{c}{24\pi}\{f(t), t\} = kE(t) \tag{4.6}$$

where

$$k = \frac{cG_N}{3\phi_r}.$$

The differential equation becomes:

$$E'(t) = \frac{\pi c}{12\beta^2} - kE(t), \tag{4.7}$$

with initial condition $E(t_0) = E_{\text{shock}} + E_{\beta} \equiv E_{\tilde{\beta}}$, where E_{shock} is the energy of the shock-wave, $\tilde{\beta}^{-1}$ is a higher temperature for the black hole gas consequence of the shockwave. Notice that for the semiclassical approximation to be valid, we need $k \ll 1$ since k sets the black hole evaporation time scale; and at the same time we need $c \gg 1$ to suppress quantum fluctuations.

The solution to (4.7) and the respective initial condition:

$$E(t) = \frac{\pi\phi_r}{4G_N}\left(\beta^{-2} + (\tilde{\beta}^{-2} - \beta^{-2})e^{-k(t-t_0)}\right) \tag{4.8}$$

which shows that the black hole settles back to a state of temperature β^{-1}, as expected from the fact that the system is coupled to a thermal bath.

4.2.2 Modified map

From Eq. (4.8), $f(t)$ can be found by solving:

$$\{f(t), t\} = -2\pi^2\left(\beta^{-2} + (\tilde{\beta}^{-2} - \beta^{-2})e^{-k(t-t_0)}\right) \tag{4.9}$$

for $t > t_0$. The solutions to the differential equation are determined up to a $SL(2, \mathbb{R})$ transformation,

$$f \to \frac{Af + C}{Bf + D},$$

where the constants A, B, C and D are fixed from continuity of the map and it's derivatives at $t = t_0$,

$$f(t_0) = \frac{\beta}{\pi} \tanh \frac{\pi t_0}{\beta}, \tag{4.10}$$

$$f'(t_0) = \operatorname{sech}^2 \frac{\pi t_0}{\beta}, \tag{4.11}$$

$$f''(t_0) = -\frac{\pi}{\beta} \sinh \frac{\pi t_0}{\beta} \operatorname{sech}^3 \frac{\pi t_0}{\beta}. \tag{4.12}$$

More detail on the solution for the differential equation subject to these initial conditions is given in the Appendix; the solution is:

$$f(t) = \frac{\beta}{\pi} \frac{K_\nu(\nu z_0)\left[\hat{f}(t)/\hat{f}(t_0) - 1\right] + z_0 \tanh \frac{\pi t_0}{\beta} \left[\hat{f}(t) I_\nu'(\nu z_0)/\alpha - K_\nu'(\nu z_0)\right]}{K_\nu(\nu z_0)\left[\hat{f}(t)/\hat{f}(t_0) - 1\right] \tanh \frac{\pi t_0}{\beta} + z_0 \left[\hat{f}(t) I_\nu'(\nu z_0)/\alpha - K_\nu'(\nu z_0)\right]}, \tag{4.13}$$

where

$$\hat{f}(t) = \alpha \frac{K_\nu(\nu z)}{I_\nu(\nu z)}, \quad \nu = \frac{2\pi}{\beta k}, \quad z = \sqrt{\frac{E_{\text{shock}}}{E_\beta}} e^{-\frac{k}{2}(t-t_0)}, \tag{4.14}$$

and α is numerical factor fixed by $\hat{f}(t_0) = e^{\frac{2\pi t_0}{\tilde{\beta}}}$.

The Bessel functions can be simplified in the high temperature limit: $\beta k \ll 1$; meaning that $\nu \gg 1$, for making the analysis easier. In this limit:

$$f(t) \simeq \frac{\beta}{\pi} \frac{\beta \tanh \frac{\pi t_0}{\beta} + \tilde{\beta} \tanh(\nu[S(t) - S(t_0)])}{\beta + \tilde{\beta} \tanh(\nu[S(t) - S(t_0)]) \tanh \frac{\pi t_0}{\beta}}. \tag{4.15}$$

$$\hat{f}(t) \simeq e^{2\nu[S(t)-S(t_0)] + \frac{2\pi}{\tilde{\beta}} t_0}, \quad S(t) \equiv -\sqrt{1+z^2} + \tanh^{-1} \frac{1}{\sqrt{1+z^2}}. \tag{4.16}$$

In particular, in the early time regime of (4.16):

$$\log \hat{f}(t) = \frac{2\pi t}{\tilde{\beta}} - \frac{\pi k(\beta^2 - \tilde{\beta}^2)}{2\beta^2 \tilde{\beta}} (t - t_0)^2 + \ldots \tag{4.17}$$

while in the late time regime $t \gg k^{-1}$,

$$\log \hat{f}(t) = \frac{2\pi}{\beta}(t + \kappa) + \ldots \tag{4.18}$$

where the dots indicate suppressed terms of the order $e^{-k(t-t_0)}$, and

$$\kappa = -\frac{2}{k} \left(1 + \log \frac{\sqrt{\beta^2 - \tilde{\beta}^2}}{2\tilde{\beta}} - \frac{k\beta t_0}{2\tilde{\beta}} - \frac{\beta}{\tilde{\beta} + \tanh^{-1} \frac{\tilde{\beta}}{\beta}} \right),$$

which shows that the black hole eventually relaxes back to the original temperature β^{-1} after long times.

Notice however, that even after the black hole returns to equilibrium, **its event horizon has shifted**. The horizon is located at $x^-_{\text{hor}} = f(\infty)$, so the original horizon (when $f(t) = \frac{\beta}{\pi}\tanh\frac{\pi t}{\beta}$) is located at $x^-_{\text{hor}} = \frac{\beta}{\pi}$, but after the horizon is behind the shockwave the map becomes (4.15), which means that the horizon is now:

$$x^-_{\text{hor}} = f(\infty) = \frac{\beta}{\pi}\frac{\tilde{\beta} + \beta\tanh\frac{\pi t_0}{\beta}}{\beta + \tilde{\beta}\tanh\frac{\pi t_0}{\beta}} < \frac{\beta}{\pi}. \tag{4.19}$$

4.2.3 Dilaton

As the shockwave enters the gravitational region, $T_{x^+x^+} \neq 0$ since:

$$T_{x^+x^+} = \frac{1}{(f'(y^+))^2}\left(\frac{\pi c}{12\beta^2} + \frac{c}{24\pi}\{f(y^+), y^+\}\right) = -\frac{\phi_r}{8\pi G_N}\partial_{x^+}f'(y^+). \tag{4.20}$$

where I have applied Eq. (4.7). Meanwhile $T_{x^+x^-} = T_{x^-x^-} = 0$ since the shockwaves enter the gravitational region, but do not leave as they become trapped in the black hole. As a result, the dilaton back-reacts according to its equations of motion, and we can find its solution behind the shockwave from Eq. (3.14):

$$\phi = 2\phi_r\left(\frac{\hat{f}''(y^+)}{2\hat{f}'(y^+)} + \frac{\hat{f}'(y^+)}{x^- - \hat{f}(y^+)}\right), \tag{4.21}$$

while behind the shockwave, ϕ is still given by Eq. (3.15).

Let's define new vacuum coordinates, $\tilde{w}^\pm$:

$$\tilde{w}^\pm \equiv \pm\hat{f}(y^\pm)^{\pm 1}. \tag{4.22}$$

Now the dilaton can be written in a simple way in the y^+, $\tilde{w}^-$ coordinates:

$$\phi = 2\phi_r\left(\frac{\hat{f}''(y^+)}{2\hat{f}'(y^+)} + \frac{\tilde{w}^-\hat{f}'(y^+)}{1 + \tilde{w}^-\hat{f}(y^+)}\right). \tag{4.23}$$

This allows to calculate the Bekenstein-Hawking entropy from $\phi/(4G_N)$ at the horizon,

$$\begin{aligned} S_{BH}(y^+) &= \frac{1}{4G_N}\left(\phi_0 + \phi_r\frac{\hat{f}''(y^+)}{\hat{f}'(y^+)}\right) \\ &= \frac{1}{4G_N}\left(\phi_0 + \frac{k\phi_r}{z}\frac{(\nu z^2 + 2(\nu-1))I_{\nu-1}(\nu z) - \nu z I_{\nu-2}(\nu z)}{I_\nu(\nu z)}\right). \end{aligned} \tag{4.24}$$

For $\beta k \ll 1$,

$$S_{BH} \to \frac{1}{4G_N}\left(\phi_0 + \frac{2\pi\phi_r}{\beta}\sqrt{1+\frac{E_{\text{shock}}}{E_\beta}e^{-k(y^+-t_0)}}\right)$$

which must be consistent with the black hole settling down to its original temperature at late times, for which we need to find $y^+(t)$ by the QES prescription in subsection 4.3.3.

4.3 Entropy calculation

Now we can compute the entropy of the radiation region; we must construct the generalized entropy and extremize in the case that there are islands, find the location of the respective QES, and find the corresponding entropy, in a similar matter to what has been performed in the previous section. However, we must take into account that as the system evolves we must consider following entropy saddle configurations: when there are no islands; and when the island appears with the QES in front, or behind the shockwave. In what follows, we shall make use of the following approximations to make the analysis simpler:

- Consider the limit $\beta k \ll 1$ to simplify the mapping.
- Consider late-times, meaning that the boundary time t is around or after the original Page time (which is astronomically big), to ignore cross terms between left and right systems, considering a CFT of free fermions, as done in [3], for the simplification that the two interval entropy computation reduces to twice the single interval case. From now on, when we mention *early times* we mean: $\frac{2\pi}{\beta}(t-t_0) \ll 1$, and late times $\frac{2\pi}{\beta}(t-t_0) \gg 1$

4.3.1 No island case

After the shockwave crosses the boundary, the map becomes:

$$w^+ = e^{\frac{2\pi}{\beta}t}, \quad w^- = -e^{-\frac{2\pi}{\beta}\eta(t)} \equiv \frac{\pi f(t)-\beta}{\pi f(t)+\beta} \tag{4.25}$$

which implies that the conformal factor in Eq. (3.21) changes to:

$$\Omega^{-2} = \frac{\beta^2}{(2\pi)^2\eta'(t)}e^{-\frac{2\pi}{\beta}(t-\eta(t))}$$

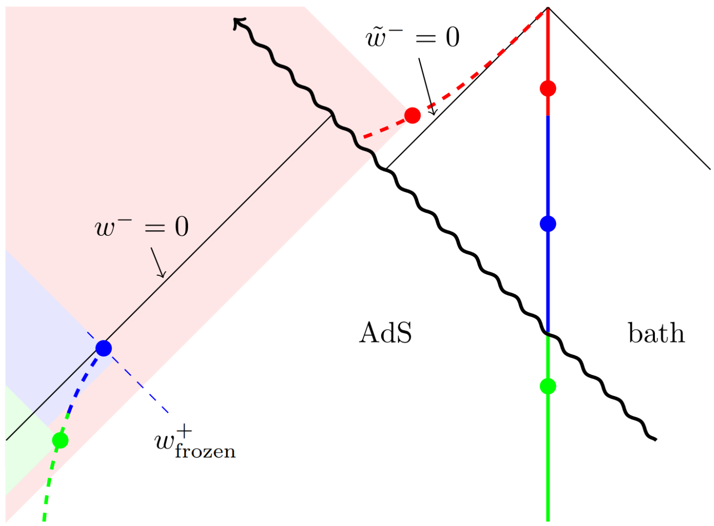

Figure 4.3: Saddle points and the corresponding boundary time (boundary points between the bath and AdS regions). The QES are blobs and the islands are shaded areas, while the boundary time appears as colored lines corresponding to the saddle that minimizes the entropy. The green and blue saddles occur when the QES is behind shockwave. The green saddle corresponds to before the shockwave crosses to the AdS region, in which case the arguments the previous section apply, namely Eq. (3.29) for $\beta k \ll 1$. In the blue case occurs after the boundary point crosses the incoming shockwave, $t > t_0$; and as boundary time increases, the QES approaches the black hole horizon, then freezes (meaning that there is no solution for the QES) after the QES reaches the horizon (at $w^- = 0$) at a particular value w^+_{freeze}. The red saddles indicates that the QES reappears and is now behind the shockwave. Eventually the QES migrates from inside to outside the horizon, as expected when the system reaches the original thermal equilibrium.

and following the same analysis of Figure 3.4, in this configuration we have $w_1^{\pm} = w_2^{\mp}$. Eq. (3.21) leads to:

$$\begin{aligned} S_{\text{no-isl}} =& \frac{c}{3}\log\left(e^{\frac{2\pi}{\beta}t} + e^{-\frac{2\pi}{\beta}\eta(t)}\right) - \frac{\pi c}{3\beta}(t-\eta(t)) - \frac{c}{6}\log \eta'(t) \\ &+ \frac{c}{3}\log\frac{\beta}{2\pi} + 2S_{\text{shock}}. \end{aligned} \tag{4.26}$$

4.3.2 Island with QES in front of the shockwave

When the boundary point crosses the shockwave, the entropy found in Eq. (3.26) is modified, and we must analyze two different cases, when the QES is in front or behind the shockwave, i.e. whether the geometry has been perturbed. As the system evolves, the QES will go from being in front of the the shockwave to be behind it. This evolution is illustrated in Figure 4.3. For the first case (QES behind the shockwave), the mapping of the coordinates changes, but the form of the dilaton does not. We may use vacuum coordinates $w^{\pm}$, as in Eq. (4.25) applied to the boundary,

$$w_2^+ = e^{\frac{2\pi}{\beta}t}, \quad w_2^- = -e^{-\frac{2\pi}{\beta}\eta(t)} \tag{4.27}$$

and the respective conformal factor. With the appearance of the island $w_1^{\pm} \neq w_2^{\mp}$, we must proceed with finding the $w_1^{\pm}$ of the QES, by extremizing the generalized entropy:

$$S_{\text{gen}}(w_1^{\pm}) = \frac{\phi_0}{2G_N} + \frac{c}{3}F(w_1^{\pm}) + \frac{c}{3}F(w_1^{\pm}) + \frac{c}{3}\log\frac{2}{\Omega_2} + 2S_{\text{shock}} \tag{4.28}$$

where

$$F(w_1^{\pm}) = \frac{\pi}{\beta k}\frac{1-w_1^+w_1^-}{1+w_1^+w_1^-} + \log\frac{\left(-w_1^+ + e^{\frac{2\pi}{\beta}t}\right)\left(w_1^- + e^{-\frac{2\pi}{\beta}\eta(t)}\right)}{1+w_1^+w_1^-}. \tag{4.29}$$

To find analytic expressions for $w_1^{\pm}$, we should use the $\beta k \ll 1$ limit, leading to

$$w_1^+ = \frac{\beta k}{2\pi}e^{\frac{2\pi}{\beta}\eta(t)}, \quad w_1^- = -\frac{\beta k}{2\pi}e^{-\frac{2\pi}{\beta}t}, \tag{4.30}$$

and the respective entropy:

$$S = 2S_{BH}^{(\beta)} + 2S_{\text{shock}} + \frac{\pi c}{3\beta}(t-\eta(t)) - \frac{c}{6}\log\eta'(t). \tag{4.31}$$

As t increases, the entropy increases. At late times, we must consider the case where the QES is behind the shockwave.

In the blue saddle region of Fig. 4.3 the QES has coordinates shown in (4.30) with $\eta(t)$ defined in (4.25). We can evaluate $\eta(t)$ by considering the limit $\beta k \ll 1$, for which Eq. (4.16) is valid; leading to

$$e^{-\frac{2\pi}{\beta}\eta(t)} = e^{-\frac{2\pi}{\beta}t_0}\frac{(\beta-\tilde{\beta})\hat{f}(t) + (\beta+\tilde{\beta})e^{\frac{2\pi}{\beta}t_0}}{(\beta+\tilde{\beta})\hat{f}(t) + (\beta-\tilde{\beta})e^{\frac{2\pi}{\beta}}}. \tag{4.32}$$

Since $\hat{f} \sim e^{\frac{2\pi}{\tilde{\beta}}t}$ at early times, then $\eta(t)$ increases linearly near t_0, and after a time

$$t \sim t_0 + \frac{\tilde{\beta}}{2\pi}\log\frac{4\beta\tilde{\beta}}{\beta^2-\tilde{\beta}^2} \tag{4.33}$$

η saturates to a constant value η_0:

$$\eta(t) \to \eta_0 = t_0 + \frac{\beta}{2\pi}\log\frac{\beta+\tilde{\beta}}{\beta-\tilde{\beta}}. \tag{4.34}$$

The QES starts on the same Cauchy slice as the boundary point, but then starts to lag behind the Cauchy slice as $\eta(t)$ saturates after the time in (4.33). Consider when the QES moves to the black hole horizon at $x^-_{\text{hor}} = f(\infty)$ given in (4.19), the QES would advance in the w^- direction, but w^+ becomes frozen at the value

$$w^+_{\text{frozen}} = \frac{\beta k}{2\pi}\frac{\beta + \pi f(\infty)}{\beta - \pi f(\infty)} = \frac{\beta k}{2\pi}\frac{\beta + \tilde{\beta}}{\beta - \tilde{\beta}} e^{\frac{2\pi}{\beta}t_0} = \frac{\beta k}{2\pi} e^{\frac{2\pi}{\beta}\eta_0}. \tag{4.35}$$

4.3.3 Island with QES behind the shockwave

At late times, the QES is behind the shockwave, and the dilaton get modified since the stress tensor changes. Let's use the $\tilde{w}$ in Eq. (4.22) as vacuum coordinates since the dilaton is easier to write down in these coordinates, and it will simply the extremization. The boundary point is at:

$$y_2^+ = t, \quad \tilde{w}_2 = -\frac{1}{\hat{f}(t)}. \tag{4.36}$$

The respective conformal factors for the QES (at $y_1^+, \tilde{w}_1^-$), and the boundary point:

$$\Omega_1^{-2} = \frac{2}{(1+\tilde{w}_1^- \hat{f}(y_1^+))^2}\frac{\beta \hat{f}'(y_1^+)}{\pi e^{\frac{2\pi}{\beta}y_1^+}}, \quad \Omega_2^{-2} = \frac{\beta(\hat{f}(t))^2}{2\pi e^{\frac{2\pi}{\beta}t}\hat{f}'(t)}. \tag{4.37}$$

Collecting these results and the expression for the dilaton in (4.23), the generalized entropy (3.26) now becomes:

$$S(y_1^+, \tilde{w}_1^-) = \frac{\phi_0}{2G_N} + \frac{c}{3}F(y_1^+, \tilde{w}_1^-) + \frac{c}{6}\log\frac{(\hat{f}(t))^2}{e^{\frac{2\pi}{\beta}t}\hat{f}'(t)} + \frac{c}{3}\log\frac{\beta}{\pi}, \tag{4.38}$$

where

$$\begin{aligned} F(y_1^+, \tilde{w}_1^-) =& \frac{1}{k}\left[\frac{\hat{f}''(y_1^+)}{2\hat{f}'(y_1^+)} - \frac{\tilde{w}_1^- \hat{f}'(y_1^+)}{1+\tilde{w}_1^- \hat{f}'(y_1^+)}\right] + \frac{1}{2}\log\frac{\hat{f}'(y_1^+)}{e^{\frac{2\pi}{\beta}y_1^+}} \\ &+ \log\frac{(-e^{\frac{2\pi}{\beta}y_1^+} + e^{\frac{2\pi}{\beta}t})(\tilde{w}_1 + 1/\hat{f}(t))}{1+\tilde{w}_1^- \hat{f}(y_1^+)}. \end{aligned} \tag{4.39}$$

Notice that the factor $2S_{\text{shock}}$ no longer appears since the region D of Fig. 3.5 does not contain the shockwave. Extremizing over $\tilde{w}_1^-$:

$$\tilde{w}_1^- = \frac{\hat{f}'(y_1^+) + k\hat{f}(y_1^+) - k\hat{f}(t)}{\hat{f}(t)(k\hat{f}(y_1^+) - \hat{f}'(y_1^+)) - k(\hat{f}(y_1^+))^2}. \tag{4.40}$$

To find analytic solutions, let's consider $\beta k \ll 1$. At early times (near t_0), we can take $\tilde{w}_1^+ = \hat{f}(y_1^+)$ and apply Eq. (4.17), to express

$$y_1^+ = \frac{\tilde{\beta}}{2\pi} \log \tilde{w}_1^+ + \frac{k\tilde{\beta}^2(\beta^2 - \tilde{\beta}^2)}{(4\pi\beta)^2} \left[\log \tilde{w}_1^+ - \frac{2\pi t_0}{\tilde{\beta}} \right]^2 + \dots \tag{4.41}$$

where the dots include higher order terms in $k\beta$. We may extremize $F(\tilde{w}_1)$ while keeping up to order $(\beta k)^0$ to find the short time behavior in the high temperature limit of

$$\tilde{w}_1^+ = \frac{k\tilde{\beta}(3\beta - \tilde{\beta})(\beta + \tilde{\beta})}{8\pi\beta^2} e^{\frac{2\pi}{\beta}t}, \quad \tilde{w}_1^- = \frac{(\beta - \tilde{\beta})^2}{(3\beta - \tilde{\beta})(\beta + \tilde{\beta})} e^{-\frac{2\pi}{\beta}t}, \tag{4.42}$$

where it is seen that $w_1^- > 0$ always, implying that the QES is inside the horizon at early times for $\beta k \ll 1$.

Sometimes it's useful to analyze the *scrambling time* of the process, we define it as the difference between current boundary time with the boundary time of an in-going null ray that just passes through the QES; it is a measure of how much is the QES lagging behind the boundary point. In this process, the scrambling time is given by:

$$\Delta t_s \equiv t - y^+. \tag{4.43}$$

At early times from Eqs. (4.41) and (4.42)

$$\Delta t_s = t - y^+ = \frac{\tilde{\beta}}{2\pi} \log \frac{8\pi\beta^2}{k\tilde{\beta}(3\beta - \tilde{\beta})(\beta + \tilde{\beta})}; \tag{4.44}$$

Δt_s indicates the minimum time that takes for quantum information thrown into a black hole to be recoverable in the Hawking radiation (which in this case, means to be inside the island), as stated in the Hayden-Preskill protocol [36].

Since the scrambling time appears only for $y_1^+ > t_0$, the early time approximation (4.44) implies that $t > t_0 + \Delta t_s$, meaning that in the the QES appears behind the shockwave about a scrambling time after the insertion of the shockwave.

On the other hand, at late times $\hat{f}(t) = e^{\frac{2\pi}{\beta}(t+\kappa)}$, as seen in Eq. (4.18). To simplify the analysis let's introduce the scrambling time of Eq. (4.43), to be able to express Eq. (4.42) as,

$$\tilde{w}_1^- = e^{-\frac{2\pi}{\beta}(t+\kappa)} \frac{k\left(e^{\frac{2\pi}{\beta}\Delta t_s} + 1\right) + \frac{2\pi}{\beta}}{k\left(1 - e^{\frac{-2\pi\Delta t_s}{\beta}}\right) - \frac{2\pi}{\beta}}. \tag{4.45}$$

The extremization condition $\partial_{y^+} F(y_1^+, \tilde{w}_1^-) = 0$ yields a simple expression for the scrambling time:

$$\sinh \frac{2\pi\Delta t_s}{\beta} = \frac{\pi}{\beta k} \tag{4.46}$$

which in the $\beta k \ll 1$ limit tells us that

$$\Delta t_s = \frac{\beta}{2\pi} \log \frac{2\pi}{\beta k}.$$

Returning to Eq. (4.40),

$$\tilde{w}_1^- = -\frac{\beta k}{2\pi} e^{-\frac{2\pi}{\beta}(t+\kappa)} \tag{4.47}$$

where we notice that $\tilde{w}_1^- < 0$. This implies that at late times, which is when the black hole is back to equilibrium, the QES is outside the horizon as before.

In other words, the longer the system is in non-equilibrium, the longer the QES should be inside the horizon.

4.4 Page curves

After finding the different cases entropy saddles corresponding to each of the cases: no-island, island with QES in front or behind the shockwave; the Page curve is the one with lowest entropy between those cases, which implies the appearance of entropy transitions.

The multiple scenarios corresponding to multiple entanglement structures that can be realized, as seen in Fig. 4.4, where we see two different scenarios, in which we observe some saddle may or may not contribute to the Page curve; which scenario is realized depends on the initial conditions such as the insertion time t_0, E_{shock}, S_{shock}. This transition is the result of a discontinuity in the entropy curve caused by the shockwave, which carries energy and entropy. Since the shockwave consists on two pulses, one thrown into the thermal bath, and the other one into the black hole, which are entangled; when the shockwave enters the black hole region, it increases the entanglement between the black hole and the radiation bath. This effect enhances the velocity to reach Page time. However, since the shockwave also carries energy, it heats up the black hole, increases its entropy, which results into a delay of the Page time. The net effect of the black hole having a shorter or longer Page time will depend on the initial parameters, as seen in Fig. 4.4.

- If the shockwave is inserted before the original Page time and the S_{shock} is small respect to the other factors contributing to the entropies in (4.26), (4.31), the transition is avoided, a new Page time emerges, and the Page time consist of the no-island saddle up to a point where the saddle has a QES behind the Page time, as in the left plot of Fig. (4.4).

- If the shockwave is inserted after the original Page time and the S_{shock} is small, saddle transitions occur, as seen in the right plot of Fig. (4.4), again a new Page time occurs.

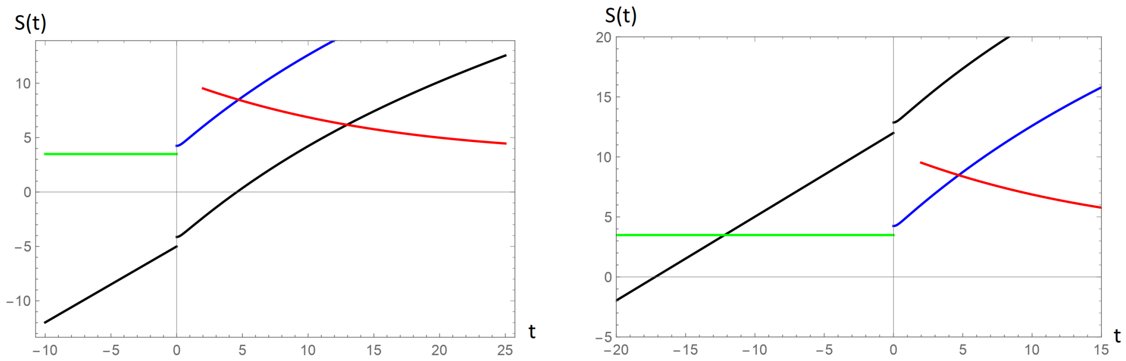

Figure 4.4: Two different scenarios for the Page curve, where the time axis is shifted to set $t_0 = 0$, and the entropy axis is shifted by convenience. The saddle that minimizes the entropy at a given time can differ depending on the initial conditions. On the left, the shock wave is thrown before the original Page time of the black hole; on the right the shock wave is thrown after the original Page time. The black curve is the no-island saddle, and the other colors have the same meaning as explained in Figure 4.3. In both cases, the red curve is the minimal one at late times (appearing a scrambling time after the insertion at $t_0 = 0$), eventually relaxing to the original equilibrium configuration.

- If S_{shock} is large, either of the previous scenarios have a delayed transition to the final saddle, given by the scrambling time.

Chapter 5

Perspectives for the future

An argument, raised on [5], that we have mentioned before is that the recent developments have captured how to do the correct entropy computation from the semiclassical geometry, but it does not give us an explicit picture for the degrees of freedom involved in the calculation, including those in the initial black hole interior and the final Hawking radiation that also includes the interior, and how is this process realized microscopically. We could learn about the degrees of freedom from the density matrix of the radiation, or the S-matrix of the black hole describing transitions between microstates. These type of concepts have been obtained when we assume particular quantum gravity theories, or holography; it would be desirable to extract information about the quantum state of Hawking radiation purely from the semiclassical picture; which would also allow us to learn about the black hole interior, since as we saw in the review, at late times, the radiation encodes information about the interior of the black hole; could this be used to extract information about the black hole singularity that we can still study with effective field theory?

As for the Euclidean path integral, the precise integration contour in the Euclidean path integral calculation should also be pursued, depending on it we might find other saddle points. N. Engelhardt pointed out that we should perform the path integral calculation purely from quantum field theory to compare the von Neumann entropy that gives the Page curve, with the obtained by Hawking [37]. This procedure should confirm our ideas between the fine-grained vs. the coarse grained entropy.

These ideas have been applied when the black hole + CFT configuration is initially in the thermofield double state, which is a very particular quantum state that happens to have a holographic dual, the results should be tested when we allow more general initial states, however the computations would become more complicated as the path integral preparation is modified. A modest approach to this problem is to consider the JT gravity + thermal bath set up, and insert local quenches in the gravitational region instead of the bath region, in order for perturbing the initial state; we would like to study the consequences in the evolution of the Page curve. We expect that the unitary evolution would hold, as it would be a modification of the Hollowood-Kumar procedure of Chapter 4, and the main difference would be the appearance of new entropy saddles, and the same late time behavior as the original set up. It would be good to compute the Page curve in more realistic black holes settings, since it is possible that replica wormholes (which proves the island rule) have no contribution to the path integral, and information is actually lost, even if it seems unlikely.

Finally, these concepts could be explored in cosmology because there is a cosmological event horizon due to accelerated expansion, which is similar to a black hole horizon; it has an associated entropy and an associated Hawking radiation [38]; but it is unclear if cosmological spacetimes can be treated quantum systems as in the central dogma [5].

Appendix A

Exact $f(t)$ and its high temperature limit

This appendix is based on [1].

A.1 Exact solution

An exact solution to the third order differential equation in (4.9) can be found in terms of modified Bessel functions, we may choose $\alpha = 1$ for convenience, to write:

$$\hat{f}(t) = \frac{K_\nu(\nu z)}{I_\nu(\nu z)} \tag{A.1}$$

where ν and z are given in Eq. (4.14). The solution to the differential equation is invariant under a Mobius transform of $\hat{f}(t)$:

$$f(t) = \frac{A\hat{f} + B}{C\hat{f} + D}.$$

The constants $A,\ B,\ C$ and D can be fixed up to a normalization factor by matching the function with the initial conditions at the insertion of the shockwave, which means imposing continuity on the mapping and its derivatives at t_0. The relevant conditions are displayed in Eqs. (4.10)-(4.12), leading to the identification

$$A = \mathcal{N} I_\nu(\nu z_0)\left[1 + z_0 \frac{I'_\nu(\nu z_0)}{I_\nu(\nu z_0)} \tanh\left(\frac{\pi t_0}{\beta}\right)\right], \tag{A.2}$$

$$B = -\mathcal{N} K_\nu(\nu z_0)\left[1 + z_0 \frac{K'_\nu(\nu z_0)}{K_\nu(\nu z_0)} \tanh\left(\frac{\pi t_0}{\beta}\right)\right], \tag{A.3}$$

$$C = \mathcal{N} \frac{\pi}{\beta} I_\nu(\nu z_0)\left[\tanh\left(\frac{\pi t_0}{\beta}\right) + z_0 \frac{I'_\nu(\nu z_0)}{I_\nu(\nu z_0)}\right], \tag{A.4}$$

$$D = -\mathcal{N} \frac{\pi}{\beta} K_\nu(\nu z_0)\left[\tanh\left(\frac{\pi t_0}{\beta}\right) + z_0 \frac{K'_\nu(\nu z_0)}{K_\nu(\nu z_0)}\right] \tag{A.5}$$

where $\mathcal{N}$ is an irrelevant normalization factor, as it cancels in the Mobius transformation, which we can fix by the condition $AD - BC = 1$:

$$\mathcal{N} = \sqrt{\frac{k}{2}} \cosh\left(\frac{\pi t_0}{\beta}\right).$$

The exact result for $f(t)$ obeying the appropriate initial conditions is shown in Eq. (4.13).

A.2 High temperature limit

In the $\beta k \ll 1$ limit, the index ν of the Bessel functions is large and we can then use integral representations for I_ν and K_ν and apply the method of steepest descent. For example for the modified Bessel function of the first kind I_ν (consider $\mathrm{Re}\,\nu > -1/2$):

$$I_\nu(\nu z) = \left(\frac{\nu z}{2}\right)^\nu \frac{1}{\sqrt{\pi}\Gamma(\nu + \frac{1}{2})} \int_0^\pi e^{\nu z \cos\theta} (\sin\theta)^{2\nu} d\theta. \tag{A.6}$$

In the $\nu \gg 1$ limit the integral is dominated by a saddle point at $\theta = 0$ and it can be evaluated as,

$$I_\nu(\nu z\,)\Big|_{\nu \gg 1} \simeq \frac{1}{\sqrt{\pi}} \exp\left[\nu\left(\sqrt{1+z^2} - \tanh^{-1}\frac{1}{\sqrt{1+z^2}}\right)\right]. \tag{A.7}$$

Similarly, for the modified Bessel function of the second kind,

$$K_\nu(\nu z) = \sqrt{\pi}\left(\frac{\nu z}{2}\right)^\nu \frac{1}{\Gamma(\nu + \frac{1}{2})} \int_0^\infty e^{-\nu z \cosh t} (\sinh t)^{2\nu} dt, \tag{A.8}$$

$$K_\nu(\nu z\,)\Big|_{\nu \gg 1} \simeq \sqrt{\pi} \exp\left\{-\nu\left(\sqrt{1+z^2} - \tanh^{-1}\frac{1}{\sqrt{1+z^2}}\right)\right\}. \tag{A.9}$$

Substituting these expressions into (A.1) leads to

$$\hat{f}(t)\Big|_{\nu\ll 1} \approx \pi\alpha \exp(2\nu S(t)), \tag{A.10}$$

where

$$S(t) = S(t_0) + \frac{\pi}{\nu}\int_{t_0}^{t} \frac{dt'}{\beta_{eff}(t')},$$

$$\beta_{eff}^{-1}(t) = \beta^{-1}\sqrt{1 + e^{-k(t-t_0)}\frac{E_{\text{shock}}}{E_\beta}}.$$

Bibliography

[1] T. J. Hollowood and S. P. Kumar, “Islands and page curves for evaporating black holes in jt gravity,” *arXiv preprint arXiv:2004.14944*, 2020.

[2] S. Lloyd, *Black Holes, Demons and the Loss of Coherence: How complex systems get information, and what they do with it*. PhD thesis, Rockefeller University, 1988.

[3] A. Ahmed, T. Hartman, M. Juan, S. Edgar, and T. Amirhossein, “Replica wormholes and the entropy of hawking radiation,” *Journal of High Energy Physics*, vol. 2020, no. 5, 2020.

[4] G. Penington, S. H. Shenker, D. Stanford, and Z. Yang, “Replica wormholes and the black hole interior,” *arXiv preprint arXiv:1911.11977*, 2019.

[5] A. Almheiri, T. Hartman, J. Maldacena, E. Shaghoulian, and A. Tajdini, “The entropy of hawking radiation,” *arXiv preprint arXiv:2006.06872*, 2020.

[6] A. Almheiri, R. Mahajan, and J. E. Santos, “Entanglement islands in higher dimensions,” *arXiv preprint arXiv:1911.09666*, 2019.

[7] T. Hartman, E. Shaghoulian, and A. Strominger, “Islands in asymptotically flat 2d gravity,” *arXiv preprint arXiv:2004.13857*, 2020.

[8] T. Anegawa and N. Iizuka, “Notes on islands in asymptotically flat 2d dilaton black holes,” *Journal of High Energy Physics*, vol. 2020, no. 7, pp. 1–14, 2020.

[9] K. Hashimoto, N. Iizuka, and Y. Matsuo, “Islands in schwarzschild black holes,” *Journal of High Energy Physics*, vol. 2020, no. 6, pp. 1–21, 2020.

[10] D. Marolf and H. Maxfield, “Transcending the ensemble: baby universes, spacetime wormholes, and the order and disorder of black hole information,” *arXiv preprint arXiv:2002.08950*, 2020.

[11] A. Almheiri, R. Mahajan, J. Maldacena, and Y. Zhao, “The page curve of hawking radiation from semiclassical geometry,” *Journal of High Energy Physics*, vol. 2020, no. 3, pp. 1–24, 2020.

[12] A. Almheiri, R. Mahajan, and J. Maldacena, "Islands outside the horizon," *arXiv preprint arXiv:1910.11077*, 2019.

[13] J. Polchinski, "The black hole information problem," in *New Frontiers in Fields and Strings: TASI 2015 Proceedings of the 2015 Theoretical Advanced Study Institute in Elementary Particle Physics*, pp. 353–397, World Scientific, 2017.

[14] J. D. Bekenstein, "Black holes and the second law," *Lettere al Nuovo Cimento (1971-1985)*, vol. 4, no. 15, pp. 737–740, 1972.

[15] J. D. Bekenstein, "Black holes and entropy," *Physical Review D*, vol. 7, no. 8, p. 2333, 1973.

[16] S. W. Hawking, "Black hole explosions?," *Nature*, vol. 248, no. 5443, pp. 30–31, 1974.

[17] S. W. Hawking, "Particle creation by black holes," *Communications in mathematical physics*, vol. 43, no. 3, pp. 199–220, 1975.

[18] S. B. Giddings, "Quantization in black hole backgrounds," *Physical Review D*, vol. 76, no. 6, p. 064027, 2007.

[19] K. Papadodimas, "Notes on holography, black holes, and quantum information." SISSA, 2020.

[20] A. C. Wall, "Proof of the generalized second law for rapidly changing fields and arbitrary horizon slices," *Physical Review D*, vol. 85, no. 10, p. 104049, 2012.

[21] S. Ryu and T. Takayanagi, "Holographic derivation of entanglement entropy from ads," *CFT, arxiv*, vol. 603001, 2016.

[22] V. E. Hubeny, M. Rangamani, and T. Takayanagi, "A covariant holographic entanglement entropy proposal," *Journal of High Energy Physics*, vol. 2007, no. 07, p. 062, 2007.

[23] T. Faulkner, A. Lewkowycz, and J. Maldacena, "Quantum corrections to holographic entanglement entropy," *Journal of High Energy Physics*, vol. 2013, no. 11, p. 74, 2013.

[24] N. Engelhardt and A. C. Wall, "Quantum extremal surfaces: holographic entanglement entropy beyond the classical regime," *Journal of High Energy Physics*, vol. 2015, no. 1, p. 73, 2015.

[25] A. Lewkowycz and J. Maldacena, "Generalized gravitational entropy," *Journal of High Energy Physics*, vol. 2013, no. 8, p. 90, 2013.

[26] T. Banks, L. Susskind, and M. E. Peskin, "Difficulties for the evolution of pure states into mixed states," *Nuclear Physics B*, vol. 244, no. 1, pp. 125–134, 1984.

[27] S. W. Hawking, "Information loss in black holes," *Physical Review D*, vol. 72, no. 8, p. 084013, 2005.

[28] A. Strominger, "Unitary rules for black hole evaporation," *arXiv preprint hep-th/9410187*, 1994.

[29] A. Almheiri, N. Engelhardt, D. Marolf, and H. Maxfield, "The entropy of bulk quantum fields and the entanglement wedge of an evaporating black hole," *Journal of High Energy Physics*, vol. 2019, no. 12, p. 63, 2019.

[30] F. Gautason, L. Schneiderbauer, W. Sybesma, and L. Thorlacius, "Page curve for an evaporating black hole," *Journal of High Energy Physics*, vol. 2020, no. 2004.00598, pp. 1–23, 2020.

[31] J. Lin, "Entanglement entropy in jackiw-teitelboim gravity," *arXiv preprint arXiv:1807.06575*, 2018.

[32] J. Maldacena and L. Susskind, "Cool horizons for entangled black holes," *Fortschritte der Physik*, vol. 61, no. 9, pp. 781–811, 2013.

[33] A. Almheiri, D. Marolf, J. Polchinski, and J. Sully, "Black holes: complementarity or firewalls?," *Journal of High Energy Physics*, vol. 2013, no. 2, p. 62, 2013.

[34] M. Nozaki, T. Numasawa, and T. Takayanagi, "Quantum entanglement of local operators in conformal field theories," *Physical review letters*, vol. 112, no. 11, p. 111602, 2014.

[35] S. He, T. Numasawa, T. Takayanagi, and K. Watanabe, "Quantum dimension as entanglement entropy in two dimensional conformal field theories," *Physical Review D*, vol. 90, no. 4, p. 041701, 2014.

[36] P. Hayden and J. Preskill, "Black holes as mirrors: quantum information in random subsystems," *Journal of high energy physics*, vol. 2007, no. 09, p. 120, 2007.

[37] N. Engelhardt, "Black hole information panel discussion." Strings 2020, 2020.

[38] G. W. Gibbons and S. W. Hawking, "Cosmological event horizons, thermodynamics, and particle creation," *Physical Review D*, vol. 15, no. 10, p. 2738, 1977.